Laminar Burning Velocity and Development of a Chemical Kinetic Model for Small Oxygenated Fuels

Christensen, Moah

2016

Document Version:
Publisher's PDF, also known as Version of record

Laminar burning velocity and development of a chemical kinetic model for small oxygenated fuels

Laminar burning velocity and development of a chemical kinetic model for small oxygenated fuels

Moah Christensen

LUND
UNIVERSITY

DOCTORAL DISSERTATION
by due permission of the Faculty engineering, Lund University, Sweden.
To be defended at Rydbergsalen, Fysicum, Professorsgatan 1, 29th of April 2016 13:00.

Faculty opponent

Professor Peter Glarborg
Technical University of Denmark, Kgs. Lyngby, Denmark

Organization LUND UNIVERSITY Division of Combustion Physics Department of Physics P.O box 118, SE-211 00 Lund, Sweden	Document name: Doctoral dissertation Date of issue March 21, 2016
Author(s) Moah Christensen	CODEN LUTFD2/TFCP-193-SE
Title and subtitle Laminar burning velocity and development of a chemical kinetic model for small oxygenated fuels	

The thesis work was performed with the aim of increasing knowledge and understanding of the combustion of oxygenated fuels and intermediates. This was accomplished in two steps: experimental measurements of the laminar burning velocity to expand current databases and development of a reaction mechanism.

In the first part of the project, the laminar burning velocity of oxygenated fuels and intermediates was measured using the heat flux method. Emphasis was placed on extending the experimental database for fuels and intermediates with limited or scattered experimental data. The laminar burning velocities of acetaldehyde and methyl formate were investigated experimentally and were compared with kinetic mechanisms from the literature.

In addition, temperature dependence of the laminar burning velocity, expressed as $S_L=S_{L0}(T/T_0)^{\alpha}$, was investigated both numerically and experimentally. It was found that a kinetic mechanism can overpredict the experimental laminar burning velocity yet still display good agreement with the experimentally determined temperature dependence. To investigate the temperature dependence further a sensitivity analysis of the α coefficient was performed. The sensitivity analysis provided a different view of the chemistry involved compared to the sensitivity of the laminar burning velocity.

In the second part of the project, a contemporary detailed kinetic mechanism for the combustion of small oxygenated fuels and intermediates was developed. The mechanism was developed with the version 0.6 of the Konnov mechanism as a starting point. Reactions involved in the combustion of formaldehyde, methanol and acetic acid were reviewed and the most reliable rate constants were selected. The new kinetic mechanism was validated against experimental data from the literature covering a wide range of conditions including shock tube and flow reactors as well as burner stabilized and freely propagating flames.

The sub mechanism for methanol and formaldehyde successfully reproduced experimental data from shock tube pyrolysis and flow reactor oxidation. The mechanism was in closer agreement with experimental data concerning the laminar burning velocity of methanol than version 0.6 of the Konnov mechanism was. Validation of the mechanism for acetic acid combustion included laminar burning velocities, measured here for the very first time by use of the heat flux method. The calculated velocities were about 3 cm/s higher than the experimental results. Further validation of the kinetic mechanism was achieved by simulating species profiles of burner stabilized acetic acid flames. While major species were reproduced successfully, minor species were either under-or-over predicted. Sensitivity analysis showed ketene to play an important role in the acetic acid combustion.

The results of this project provide the scientific community with experimental data potentially useful for model validation as well as a new kinetic mechanism for small oxygenated fuels and intermediates.

Key words Oxygenated fuels, Kinetic mechanism, Validation, Sensitivity, Laminar burning velocity , Heat flux method		
Classification system and/or index terms (if any)		
Supplementary bibliographical information		Language English
ISSN and key title ISSN 1102-8718		ISBN: 978-91-7623-739-7 (print) ISBN : 978-91-7623-740-3 (electronic)
Recipient's notes	Number of pages 200	Price
	Security classification	

Laminar burning velocity and development of a chemical kinetic model for small oxygenated fuels

Moah Christensen

LUND
UNIVERSITY

Faculty of Engineering | Department of Physics

ISBN 978-91-7623-739-7 (print)
ISBN 978-91-7623-740-3 (electronic)
ISSN 1102-8718
ISRN LUTFD2/TFCP-193-SE
Printed in Sweden by Media-Tryck, Lund University
Lund 2016

"We choose to go to the moon in this decade and do the other things, not because they are easy, but because they are hard."

J. F. Kennedy, 1962

Abstract

The thesis work was performed with the aim of increasing knowledge and understanding of the combustion of oxygenated fuels and intermediates. This was accomplished in two steps: experimental measurements of the laminar burning velocity to expand current databases and development of a reaction mechanism.

In the first part of the project, the laminar burning velocity of oxygenated fuels and intermediates was measured using the heat flux method. Emphasis was placed on extending the experimental database for fuels and intermediates with limited or scattered experimental data. The laminar burning velocities of acetaldehyde and methyl formate were investigated experimentally and were compared with kinetic mechanisms from the literature.

In addition, temperature dependence of the laminar burning velocity, expressed as $S_L=S_{L0}(T/T_0)^{\alpha}$, was investigated both numerically and experimentally. It was found that a kinetic mechanism can overpredict the experimental laminar burning velocity yet still display good agreement with the experimentally determined temperature dependence. To investigate the temperature dependence further a sensitivity analysis of the α coefficient was performed. The sensitivity analysis provided a different view of the chemistry involved compared to the sensitivity of the laminar burning velocity.

In the second part of the project, a contemporary detailed kinetic mechanism for the combustion of small oxygenated fuels and intermediates was developed. The mechanism was developed with the version 0.6 of the Konnov mechanism as a starting point. Reactions involved in the combustion of formaldehyde, methanol and acetic acid were reviewed and the most reliable rate constants were selected. The new kinetic mechanism was validated against experimental data from the literature covering a wide range of conditions including shock tube and flow reactors as well as burner stabilized and freely propagating flames.

The sub mechanism for methanol and formaldehyde successfully reproduced experimental data from shock tube pyrolysis and flow reactor oxidation. The mechanism was in closer agreement with experimental data concerning the laminar burning velocity of methanol than version 0.6 of the Konnov mechanism was. Validation of the mechanism for acetic acid combustion included laminar burning velocities, measured here for the very first time by use of the heat flux method. The

calculated velocities were about 3 cm/s higher than the experimental results. Further validation of the kinetic mechanism was achieved by simulating species profiles of burner stabilized acetic acid flames. While major species were reproduced successfully, minor species were either under-or-over predicted. Sensitivity analysis showed ketene to play an important role in the acetic acid combustion.

The results of this project provide the scientific community with experimental data potentially useful for model validation as well as a new kinetic mechanism for small oxygenated fuels and intermediates.

Populärvetenskaplig sammanfattning

Sedan 1900-talets början har jordens medeltemperatur ökat med ca 0.9 grader, vilket bland annat resulterat i mer extremt väder, varmare världshav och att världens isar smälter med översvämningar av kustregioner som följd. Det är numera accepterat att denna temperaturökning med stor sannolikhet beror på människans utsläpp av växthusgaser, ex koldioxid (CO_2). Koncentrationen av CO_2 i atmosfären har ökat med 40 % sedan förindustriell tid. Detta beror till stor del på förbränning av fossila bränslen. För att minska den mänskliga påverkan på klimatet måste utsläppen av växthusgas minskas. Då transportsektorn står för en stor del av utsläppen, är detta ett område där förändring kan ha stor nytta. Ett av de sätt som utforskas är att övergå till så kallade biobränslen.

Biobränslen

På senare tid har biobränslen som etanol och biodiesel blivit populär4 alternativ till fossila bränslen. Etanol kan framställas av socker eller stärkelserika växter som majs, och biodiesel kan göras av vegetabiliska oljor. Det biobränslen har gemensamt är att de är framställda av material från växtriket. Detta gör biobränslen koldioxidneutrala, då växterna under sin livstid absorberar samma mängd CO_2 från atmosfärensom släpps ut när de förbränns. Nettoutsläppet blir i teorin noll.

Biobränsleförbränning är en process som vi fortfarande vet relativt lite om. Det är viktigt att kartlägga förbränningsprocessen, inte bara för att förstå bildandet och försvinnandet av föroreningar utan även för att kunna optimera förbränningen och framställa effektivare, mer bränslesnåla, motorer som minskar utsläppen. Detta doktorandprojekt handlar om att utveckla en detaljerad modell som skall kunna simulera olika förbränningsprocesser av mindre biobränslen. Detta hoppas vi ska leda till en djupare förståelse.

Förbränning

Förbränning är en komplex kemisk process. Ofta brukar man säga att ett bränsle, exempelvis metan (CH_4), reagerar med ett oxidationsmedel, exempelvis syre (O_2), och bildar koldioxid och vatten (H_2O). Detta kan skrivas som $CH_4+O_2=CO_2+H_2O$. Men detta är en betydande förenkling: i själva verket består processen av allt från ett 30-tal till tusentals olika

reaktioner mellan olika ämnen beroende på bränsle. För att kunna simulera olika förbränningsprocesser som en flamma, så behöver man ta hänsyn till alla reaktioner som kan ske. Detaljerade modeller kan användas för att verifiera olika teorier eller för att simulera förbränning vid mycket höga tryck eller temperaturer; där det är svårt att genomföra experiment.

För att detaljerade modeller skall kunna användas för att förutspå vad som kan ske i nya förbränninsprocesser är det viktigt att modellerna är validerade. Det innebär att modellerna måste kunna simulera resultat från förbränningsprocesser i olika typer av förbränningsmiljöer med tillräcklig precision. Exempel på sådana variationer i förbränningsmiljöer kan innefatta antändningsfördröjning, olika typer av flammor, pyrolys (förbränning utan syre) och oxidation av ett bränsle.

Flamhastigheten

En av de viktigaste parametrarna i förbränning är flamhastigheten, och det är därför viktigt att våra modeller kan simulera den på ett tillfredsställande sätt. Flamhastigheten är den hastighet som flamman möter den omgivande gasen med. Denna parameter är bränslespecifik och beror på temperatur, tryck samt förhållandet mellan bränsle och syre (ekvivalenskvot, ϕ). Genom att studera flamhastigheten kan man lära sig om bränslets reaktivitet. Flamhastigheten är en viktig förbränningsegenskap och flera olika metoder utvecklats för att mäta den.

I dagsläget används framförallt tre metoder för att bestämma flamhastigheten experimentellt. Två av dessa metoder bygger emellertid på extrapolering av data för att bestämma flamhastigheten, vilket ger en ökad osäkerhet i resultaten. Den metod som används på Lunds Universitet är *heat flux*-metoden. Heat flux-brännaren möjliggör det stabilisering av flamman under ideala förhållanden, vilket gör att vi kan mäta flamhastigheten direkt utan extrapolering.

Utvecklandet av kemiska modeller är beroende av att experimentell data finns. Detta gäller inte bara för bränslet i sig utan även för andra ämnen som bildas under förbränningsprocessen, så kallade intermediat. Därför har en stor del av detta doktorandprojekt avsatts för att bestämma flamhastigheten för bränslen som sedan tidigare saknade experimentell data. Det slutgiltiga syftet med detta är att möjliggöra utvecklandet av en ny modell som kan valideras mot dessa nya data.

Modellutveckling

För att skapa en modell samlar man alla reaktioner av intresse i en reaktionsfil. Utifrån tidigare forskning kan vi identifiera de mest pålitliga hastighetskonstanterna för dessa reaktioner. Hastighetskonstanten bestämmer hur snabbt en reaktionen sker och är antingen experimentellt

bestämd eller beräknas med hjälp av kvantberäkningar. Vi kan sedan validera modellen mot data från en mängd olika experiment genom att jämföra förutsägelserna från modellen mot faktisk experimentell data. Skillnader mellan experimenten och simuleringen kan dels jämföras direkt eller undersökas med en känslighetsanalys. Denna visar vilka reaktioner som är mest känsliga och som man bör vara extra noggrann med att välja hastighetskonstant för.

Fokus för detta arbete

För att bättre förstå förbränning av biobränslen, så har detta avhandlingsarbete ett tvådelat fokus: dels att experimentellt som syftar till att bestämma flamhastigheten av biobränslen, samt ett teoretiskt som syftar till att utveckla en kemisk modell som beskriver denna förbränning.

Vi har valt att fokusera på ett par bränslen med liknande kemiska egenskaper. Alla är så kallade C_1-C_2 bränslen, och har gemensamt att de består av en-två kolatomer och har syre som en del av deras struktur. De studeranden ämnen är viktiga för förbränningsprocessen, antingen som ett bränsle i sig själv eller som viktiga intermediat.

I denna studie utvecklar vi en ny modell för att studera dessa ämnens förbränningsprocess. Den nya modellen är validerad mot flera olika experimentella data inklusive de nya resultaten från denna studies experiment.

Framtid

Om vi vill leva i en värld där förbränning leder till mindre utsläpp av farliga föroreningar och växthusgaser samtidigt som vi vill bibehålla effektiviteten i förbränningen, måste vår kemiska förståelse av förbränning fortsätta utvecklas. I jakten på full förståelse måste nya experimentella data presenteras för fler intermediat involverade i förbränningen av biobränslen. Modeller är också beroende av hastighetskonstanter, här saknas det också mycket information. Vi har i denna studie bidragit med experimentella data som kan användas för även framtida validering.

List of papers

The thesis is based on the work presented in the following papers.

Paper I. M. Christensen, M.T. Abebe, E.J.K. Nilsson, A.A. Konnov. Kinetics of premixed acetaldehyde + air flames, Proceedings of the Combustion Institute, 2015, 35(1), 499–506. Doi:10.1016/j.proci.2014.06.136

Paper II. M. Christensen, E.J.K. Nilsson and A.A. Konnov. The Temperature Dependence of the Laminar Burning Velocities of Methyl Formate + Air Flames, Fuel, 2015, 157, 162–170. Doi:10.1016/j.fuel.2015.04.072

Paper III. M. Christensen, E.J.K. Nilsson and A.A. Konnov. A systematically updated detailed kinetic model for CH_2O and CH_3OH combustion, under review in Energy & Fuels

Paper IV. M. Christensen and A.A. Konnov. Laminar burning velocity of acetic acid + air flames
Under review in Combustion and Flame

Related work

1. V.A. Alekseev, J.D. Nauclér, M. Christensen, E.J.K. Nilsson, E.N. Volkov, L.P.H. de Goey, A.A. Konnov. Experimental uncertainties of the heat flux method for measuring burning velocities, Combustion Science and Technology. 2015. Doi: 10.1080/00102202.2015.1125348

2. V.A. Alekseev, M. Christensen, A.A. Konnov. The effect of temperature on the adiabatic burning velocities of diluted hydrogen flames: A kinetic study using an updated mechanism, Combustion and Flame, 2015, 162(5), 1884–1898. Doi:10.1080/00102202.2015.1125348

3. M. Jonsson, A. Ehn, M. Christensen, M. Aldén, and J. Bood, Simultaneous one-dimensional fluorescence lifetime measurements of OH and CO in a premixed flame, Applied Physics B, 2014, 115(1), 35-43. Doi:10.1007/s00340-013-5570-7

4. J. Vancoillie, M. Christensen, E.J.K. Nilsson, S. Verhelst, A.A. Konnov. The effects of dilution with nitrogen and steam on the laminar burning velocity of methanol at room and elevated temperatures, Fuel, 2013, 105 732-738. Doi:10.1016/j.fuel.2012.09.060

5. J.F. Yu, R. Yu, X.Q. Fan, M. Christensen, A.A. Konnov, X.S. Bai. Onset of cellular flame instability in adiabatic CH4/O2/CO2 and CH4/air laminar premixed flames stabilized on a flat-flame burner, Combustion and Flame, 2013, 160(7), 1276–1286. Doi:10.1016/j.fuel.2012.09.060

6. J. Vancoillie, M. Christensen, E.J.K. Nilsson, S. Verhelst, A.A. Konnov. Temperature Dependence of the Laminar Burning Velocity of Methanol Flames. Energy & Fuels, 2012, 26 (3) 1557-1564. Doi:10.1021/ef2016683

7. J.D. Nauclér , M. Christensen, E.J.K. Nilsson, and A.A. Konnov. Oxy-fuel Combustion of Ethanol in Premixed Flames, Energy & Fuels, 2012, 26(7), 4269–4276. Doi: 10.1021/ef3008085

Table of contents

1 Introduction

The work described in the thesis was carried out with two major aims:

1) To extend the experimental database for kinetic mechanism validation by measuring the laminar burning velocity of fuels with limited or scattered data available.

2) To develop a contemporary detailed kinetic mechanism for small oxygenated fuels and intermediates through use of unmodified rate constants obtained from the literature.

Through these two aims, we can obtain a deeper understanding of detailed kinetic mechanisms for use in combustion modelling. In Papers I and II emphasis was placed on measuring the laminar burning velocity of acetaldehyde and methyl formate. These are two intermediates with previously published laminar burning velocity results that are unreliable and scattered respectively. The experimental velocities obtained were compared with kinetic mechanisms from the literature. Both papers include studies of the temperature dependence of the laminar burning velocity, expressed as $S_L=S_{L0}(T/T_0)^{\alpha}$. In Paper II it was demonstrated that two kinetic mechanisms predicting different laminar burning velocities can nevertheless display similar temperature dependence. This was investigated further by performing a sensitivity analysis of the α coefficient. To the author's knowledge, this is the first time that such a sensitivity analysis has been conducted.

In Paper III and IV a new contemporary detailed kinetic mechanism for formaldehyde, methanol and acetic acid is presented. The papers include a detailed discussion regarding the development process, selection of rate constants and reactions important for the combustion of these species. The kinetic mechanism was validated over a wide range of experimental conditions and methods, including shock tube and flow reactors, as well as burner stabilized and freely propagating flames. Sensitivity analysis was used to evaluate the importance of various reactions, and to explain certain discrepancies between experimental data and calculations.

1.1 Kinetic models in combustion

Chemical kinetic models, also referred to as mechanisms, have been used in combustion science since the late 1970s. From early on in that period, various kinetic mechanisms were used to test theories about the underlying chemistry behind combustion phenomena [1-3]. With increased availability of kinetic data and improved techniques for determination of rate constants, more accurate kinetic mechanisms were generated, able to successfully reproduce large amounts of experimental data such as the laminar burning velocity and ignition delay time. Mechanisms could then be used to predict the combustion behavior under conditions that were challenging from an experimental point of view, such as those of high temperature and/or pressure. Today detailed kinetic mechanisms play an even greater role in the study of combustion by providing chemical insight into the formation and consumption of pollutants, aiding in reducing hazardous emissions and increasing energy yields.

A chemical kinetic model consists of a reaction mechanism that includes the elementary reactions involved in the combustion of the fuel, as well as both transport and thermodynamic data of all the species involved. Associated with each reaction is a rate constant, describing how rapidly the reaction proceeds. A rate constant is either experimentally or theoretically determined and some level of uncertainty is associated with it. Mechanisms that tune rate constants within the uncertainty limits, so as to obtain a closer fit to the experimental results are called optimized, as opposed to non-optimized mechanisms that rely on unmodified rate constants.

The combustion process of a fuel can be described in terms of a sequential fragmentation of the molecule into smaller intermediate species. Consequently, kinetic mechanisms are constructed in a sequential manner [1-3]. The oxidation of hydrogen (H_2) and of carbon monoxide (CO) play important parts in the combustion of hydrocarbons and their subsets will act as a foundation for larger fuels kinetic mechanisms. From this point, the reaction mechanism is extended by adding subsets of C_1 species, such as methane (CH_4) followed by larger carbon species. Ideally, a detailed mechanism should include all the reactions of importance for the fuel in question, including reaction pathways for intermediates. The goal here is to produce a kinetic mechanism that accurately reflects the combustion chemistry involved.

Validation of the kinetic mechanism can be made for a specific range of conditions (e.g. low temperature or shock tube conditions) or for a wide range of temperatures, pressures and species concentrations reflecting real life combustion environments. This requires comparisons with data from different experimental

methods such as flow reactors, and shock tubes, and flames [1]. A mechanism validated over a wide range of conditions is referred to as being comprehensive.

The laminar burning velocity, S_L, is a combustion parameter frequently used for model validation. This fundamental, fuel-specific property is a function of the pressure, temperature and air-to-fuel ratio, ϕ. The laminar burning velocity provides information on the diffusivity, exothermicity and reactivity of the fuel and oxidizer mixture [4] and is important for turbulent combustion simulations [5]. Despite it being such a useful parameter for validation, there is a lack of reliable data or even of any data at all for some fuels and intermediates.

The work that resulted in the thesis is based on oxygenated compounds, which are molecules containing oxygen as a part of their chemical structure. The reasons for focusing on species of this type are twofold. First, oxygenated biofuels such as ethanol (C_2H_5OH) or biodiesel have become increasingly popular. This is because of their lower greenhouse gas emissions as compared with fossil fuels [6], to the economic growth associated with their use [7] and to the energy security they provide [8]. Yet combustion of these fuels is not fully understood. The diversity of oxygenated biofuels, from alcohols to biodiesel, adds additional complications, since the combustion processes involved differ. Second, combustion of hydrocarbons generates oxygenated intermediates, such as formaldehyde (CH_2O) or acetic acid (CH_3CO_2H). These two pollutants are harmful to human health and to the environment [9-11], and it is thus highly important to understand both their formation and their consumption so as to be able to reduce emissions of them. Detailed kinetic mechanism can be a useful tool to address both of these issues.

1.2 Outline of thesis

The next chapter provides the reader with some basic combustion theory important here. Specific definitions of various terms to later be made use of will be presented together with certain details about the combustion process in general. In Chapter 3, chemical kinetics and modelling will be explained. Information in that chapter can be helpful in providing an understanding of both the modelling development and simulation processes. In Chapter 4, matters concerned with the laminar burning velocity will be discussed. Experimental methods, including the heat flux method, for measuring the laminar burning velocity will be described. A closer look at the temperature dependence of the laminar burning velocity will be provided there as well. Chapters 5-6 will highlight some of the most important results from obtained in the PhD project. In Chapter 5, new experimental data concerning the laminar burning velocity of acetaldehyde and methyl formate are presented, including results

pertinent to their temperature dependence. In Chapter 6, the new kinetic mechanism developed for methanol, formaldehyde and acetic acid combustion is presented, together with validation experiments and an overview of important reactions that are involved. Lastly, Chapter 7 summarizes the thesis.

2 Basic combustion theory

Combustion, commonly defined as rapid chemical reactions between a fuel and an oxidizer, that generates heat, is a complicated process. In this chapter some basic elements of combustion theory will be presented so as to highlight and explain some of the concepts, parameters and processes that are referred to in the thesis.

2.1 Stoichiometry and equivalence ratio

Ideal combustion occurs when there is a balance between the fuel and the oxidizer so that complete conversion of the reactants to carbon dioxide (CO_2) and water (H_2O) take place. For methane reacting with oxygen (O_2), this can be written as:
$1CH_4+2O_2=1CO_2+2H_2O$
Complete combustion is preferable since this result in maximum energy being obtained from the available fuel. Due to heat loss, however this is often impossible to achieve this in real life combustion applications. A balanced mixture, with an ideal ratio of fuel to O_2 is referred to as being stoichiometric. A common way of relating the concentration of the fuel to that of the oxidizer is the equivalence ratio, ϕ. This is defined as the ratio of the fuel-to-oxidizer ratio in a mixture to the stoichiometric fuel-to-air ratio, as described in Equation (1).

$$\phi = \frac{\left(\frac{fuel}{O_2}\right)_{mix}}{\left(\frac{fuel}{O_2}\right)_{stoich}} \quad (1)$$

If there is an abundance of fuel, the mixture is termed fuel-rich, whereas if there is an excess of oxygen the mixture is termed fuel-lean. Under stoichiometric conditions the equivalence ratio is equal to 1, whereas under fuel-rich conditions $\phi>1$ and under fuel-lean conditions $\phi<1$. Examples of fuel-rich and fuel-lean conditions of methane are shown below.
$1.4CH_4+2O_2=1CO_2+2H_2O+0.4CH_4$ fuel-rich ($\phi=1.4$)
$1CH_4+3O_2=1CO_2+2H_2O+1O_2$ fuel-lean ($\phi=0.67$)

2.2 Biofuels and oxygenates

The combustion of fossil fuels has a negative impact on the environment, most notably through CO_2 emissions contributing to climate change [12]. Efforts to reduce CO_2 emissions have led to biofuels becoming attractive candidates for use as alternative fuel sources. These are fuels produced from biomass that have zero net CO_2 emissions. It has been suggested that oxygenated biofuels such as methanol (CH_3OH) and ethanol be used to replace transportation fuels or be used as fuel additives. Oxygenates are molecules containing oxygen as a part of their chemical structure. Studies have shown that oxygenated fuels are associated with lower soot formation, lower particulate emission and lower levels of unburned hydrocarbons [6, 11, 13, 14] than fossil fuels. A reduction in unburned hydrocarbon emissions is desirable since these are precursors for ground level ozone [15], which is hazardous for humans and can potentially cause premature death [16]. One drawback of oxygenated fuels, however, is their higher degree of emission of aldehydes. Formaldehyde is a major intermediate of methanol combustion, whereas acetaldehyde is the dominant species in the combustion of ethanol. Aldehydes and other oxygenated pollutants reduce the air quality as they are toxic and act as precursors to urban smog [11, 17].

2.3 Radical reactions

The conversion of a fuel and oxidizer to carbon dioxide and water does not occur in one single reaction step. Instead, there can be hundreds or even thousands of reactions involved, where intermediate species are produced and consumed. Some of these species are termed radicals which are highly reactive and play a central role in combustion processes. Reactions that create radicals from stable species are termed *chain initiation*, the radicals involved can proceed to react with other stable species resulting in one or two new radicals, in what are labeled *chain propagation* and *chain branching* respectively. If a reacting radical instead generates only stable species, the overall reactivity decreases, and the reaction in question being termed *chain terminating*. Radicals such as atomic hydrogen (H), atomic oxygen (O), the hydroxyl radical (OH), the hydroperoxyl radical (HO_2) and the formyl radical (HCO) are common in combustion. The following are examples of the different types of reactions involved:

$H_2+O_2=OH+OH$	Chain initiating
$H_2+OH=H_2O+H$	Chain propagating
$H+O_2=OH+O$	Chain branching
$H+H+M=H_2+M$	Chain terminating

2.4 Reaction pathways

The oxidation of a fuel is often initiated by hydrogen abstraction by a radical such as H, O or OH. The following is an example of a hydrogen abstraction reaction from methanol:

$CH_3OH+OH=CH_2OH+H_2O$

This reaction forms a stable water molecule and the hydroxymethyl radical (CH_2OH). The CH_2OH radical can decompose either through reacting with a third body (M) or reacting with oxygen forming formaldehyde as described by

$CH_2OH+M=CH_2O+H+M$

$CH_2OH+O_2=CH_2O+O_2$

Note that the third body, M, is not itself consumed. In the case of hydrocarbon combustion, formaldehyde is located on the main oxidation pathway to CO and CO_2. A simplified version of the oxidation pathway of methanol is shown in Figure 1.

$$CH_3OH \longrightarrow CH_2OH \longrightarrow CH_2O \longrightarrow HCO \longrightarrow CO \longrightarrow CO_2$$

Figure 1. A simplified scheme of methanol oxidation

In the absence of radicals, the initiation process involves decomposition of the fuel molecule e.g. in the form of

$CH_3OH+M=CH_3+OH+M.$

This process is slow as compared to radical reactions. The reactivity does not become significant until a pool of radicals has been established, the chain branching and propagating reactions proceeding then as described above.

The reaction pathways discussed are simply examples of what can occur. In reality, the reaction between two reactants can go through different product channels. One example is the reaction between CH_3OH and OH, which results in either CH_2OH+H_2O or $CH_3O+ H_2O$. In principal, the larger the molecule, the more complex the reaction pathway becomes. C_2 species, such as ethane (C_2H_6), have more complex oxidation pathways than C_1 species. The hydrogen abstraction of C_2H_6 results in C_2H_5 which can react, for example, to form either ethylene (C_2H_4), acetaldehyde (CH_3CHO), formaldehyde or methyl radicals (CH_3). Each of these species will have their own reaction pathway.

3 Chemical kinetics and modelling

In this chapter information relevant for the modelling part of the thesis is presented. First, various definitions and underlying theory regarding rate constants are provided. This is followed by a brief description about different experimental systems and of specific details concerning simulations of these.

3.1 Rate constants

The reaction rate of a chemical reaction is the change of a reactant or of a product concentration over time. For the reaction aA+bB=cC+dD, the reaction rate law can be expressed as in (2). In the expression, the lower case letters are the stoichiometric coefficients, the capital letters are the concentration and k is the rate constant.

$$Rate = -\frac{1}{a}\frac{\Delta[A]}{\Delta t} = -\frac{1}{b}\frac{\Delta[B]}{\Delta t} = \frac{1}{c}\frac{\Delta[C]}{\Delta t} = \frac{1}{d}\frac{\Delta[D]}{\Delta t} = k[A]^a[B]^b \quad (2)$$

The rate constant can be described in terms of the modified Arrhenius law shown in (3). In the expression, A is the pre-exponential factor, Ea the activation energy, n is a constant representing the temperature dependence, T the temperature and R is the gas constant.

$$k = AT^n e^{\left(\frac{Ea}{RT}\right)} \quad (3)$$

The unit of the rate constant is dependent upon the overall reaction order, determined by the sum of the exponents a and b in Equation (2). A first order reaction has the unit s^{-1}, a bimolecular reaction the unit $cm^3mole^{-1}s^{-1}$, and a third-order reaction has the unit $cm^6mole^{-2}s^{-1}$.

The Arrhenius expression is often derived by the fitting of experimental data, or calculated theoretically in a specific temperature range. Care should be taken in extrapolating to temperatures outside this range as the rate constant does not necessarily follow the Arrhenius expression.

Pressure dependent reactions, such as the unimolecular reaction of AB+M=P+M, where M represents a third body are examples of when the reaction rate fails to follow the Arrhenius expression. A simple mechanism describing this process was provided by Lindemann [18, 19] and will be outlined briefly. In the first step, the reactant, AB, collides with a third body resulting in AB becoming energized, AB*. In the second step of the process, the excited molecule can either de-excite back to AB or rearrange into products, P.

(R1) AB+M→AB*+M

(R-1) AB*+M→AB+M

(R2) AB*→P

The unimolecular rate constant, k_{uni}, of this process can be described by Equation (4):

$$\frac{dP}{dt} = \frac{k_1 k_2 [M]}{k_{-1}[M] + k_2}[AB] = k_{uni}[AB] \tag{4}$$

There are two limiting cases, when the pressure is very low, [M]→0 and when the pressure is very high, [M]→∞, thus resulting in two different rate constant expressions:

$$k_0 = k_1[AB][M] \tag{5}$$

$$k_\infty = \frac{k_1 k_2}{k_{-1}}[AB] \tag{6}$$

Figure 2 presents the characteristic behavior of the unimolecular rate constant with pressure. It can be clearly seen that for low pressures, the rate constant follows a linear trend. For increasing pressures, however, the rate constant starts to "fall-off" from the trend line and at sufficiently high pressures it becomes independent on pressure.

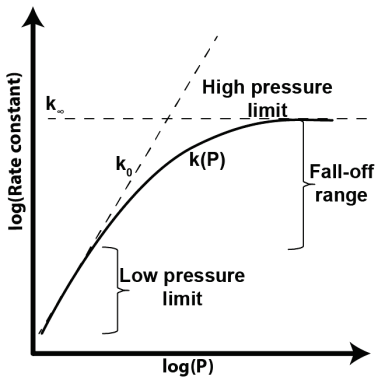

Figure 2. Pressure dependence of a unimolecular rate constant.

The Troe formalism [20] can be used to describe the reaction in the fall off region. This involves use of the high and the low pressure rate constants as described by the Arrhenius expression, shown in Equation (3). The rate constant at any given pressure can then be calculated by (7), in which P_r is the reduced pressure as defined by (8) and F being the broadening factor as described by Troe [20].

$$k = k_\infty \left(\frac{P_r}{1 + P_r}\right) F \tag{7}$$

$$P_r = \frac{k_0[M]}{k_\infty} \tag{8}$$

3.2 Modelling

Modelling was performed using the Chemkin software package [21]. This consists of several independent programs that facilitate the modeling of chemically reacting flows. Three input files are required to run simulations: a reaction mechanism which contains all the species and the reactions that are to be considered in the solution and a transport file and thermodynamic data file. The following systems have been simulated in the thesis.

3.2.1 Shock tube: method and simulations

Shock tubes are used to investigate the conversion of reactants to products and intermediate species during pyrolysis or oxidation. The method is also used to investigate the ignition delay time, τ, characterized by a strong increase in temperature and in pressure.

The shock tube consists of a long tube divided into a high-pressure (the driver section) and low pressure section (the driven section) separated by a diaphragm [22]. When the diaphragm bursts open, a shockwave will propagate through the low pressure section. The test gas in the driven section is compressed and heated to combustion temperatures through both the initial and the reflected shock. Following the reflected shock, constant volume and adiabatic conditions are assumed. Laser diagnostics can be used to measure the concentration of different species [23].

Shock tube experiments were simulated using the homogeneous batch reactor in Chemkin under constant volume and adiabatic conditions. The ignition delay time can be defined in various ways, such as maximum OH concentration or pressure. In order to successfully compare simulations to the experiments, the experimental definition needs to be implemented in the data processing.

3.2.2 Flow reactor: method and simulations

Flow reactors [23] are frequently utilized to investigate chemical kinetics as the reactions can occur under controlled conditions. The initial homogenous fuel and oxidizer mixture is injected into the reactor and the conversion that takes place can be followed as a function of different parameters such as time or temperature. Product analysis can be achieved by use of gas chromatography. Figure 3 presents typical species profiles as a function of time in a flow reactor experiment. An important parameter of the reactor is the residence time, τ, which is defined as the ratio of the volume of the reactor, V, to the flow rate of the gas through the reactor, Q.

The homogeneous batch reactor in Chemkin was used for flow reactor simulations and constant pressure and adiabatic conditions being assumed. In order to compare simulated profiles with experimental data, a time-shifting procedure [24] was performed. This is needed since there may be a radical pool buildup under the experimental conditions in the mixing region, resulting in a region of inhomogeneous concentrations. In addition, impurities in the reactants and surface reactions can affect the experiment, making it difficult to define the initial reaction time. For this reason simulated species profiles were shifted to the point at which 50 mole % of the initial experimental fuel concentration had been consumed.

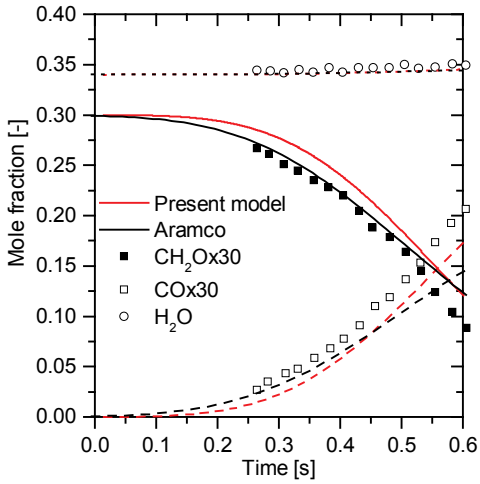

Figure 3. Examples from Paper III showing experimental and simulated species profiles from a flow reactor.

3.2.3 Jet stirred reactor: method and simulations

Jet stirred reactors, JSR, can be used for gas phase kinetic studies [25]. Mixing of the gas is achieved by use of powerful jets, resulting in a homogenous temperature and homogeneous concentrations inside the reactor. The rapid mixing causes the conversion process of reactants to products to be kinetically controlled since the mixing is faster than the chemical reactions. Gas sampling can be achieved by gas chromatography.

To simulate the experimental results of a JSR, the perfectly stirred reactor module, PSR, in Chemkin was utilized. The residence time was set to the same as the experiments.

3.2.4 Burner stabilized flames: method and simulations

The chemical reactions inv1olved in the oxidation and decomposition of a fuel can be investigated using burner stabilized flames and the experimental results are frequently used for model validation. The flames are often stabilized at low pressures (usually in the order of 10-100 mbar) in order to widen the reaction zone, thus increasing the measurement possibilities [6]. Gas sampling can be achieved using molecular beam mass spectroscopy (MBMS). Inserting the MBMS probe into the flame distorts the flow field, and acts as a heat sink, disturbing the temperature profile and subsequently the species mole fraction profiles introducing an uncertainty in the

results [26]. Differences between perturbed and non-perturbed temperature profiles have been shown to be as great as 400 K [26]. Dooley et al. [27] suggested that a 200 K discrepancy in comparison with an unperturbed flame yields modeling results that are within the limits set by the experimental error bars. Typical species profiles of a burner stabilized acetic acid flame are shown in Figure 4.

Since burner stabilized flames are not adiabatic, the temperature of the flames needs to be measured in order to be able to compare the experimental data with corresponding simulations. The temperature can be measured using different techniques such as laser diagnostics or use of thermocouples. The latter is associated with uncertainties such as radiative heat losses and flow distortion that clearly affect the accuracy of the experimental result obtained.

Simulations of the burner stabilized flames were performed using the burner stabilized flame module in Chemkin, taking thermal diffusion and multicomponent transport into account. The experimental temperature profile and gas flow were used as input parameters. The numerical solution is generally more accurate the more grid points that are included in the solution. In flame simulations a grid-independent solution was ensured by setting the parameters GRAD and CURV to sufficiently small values.

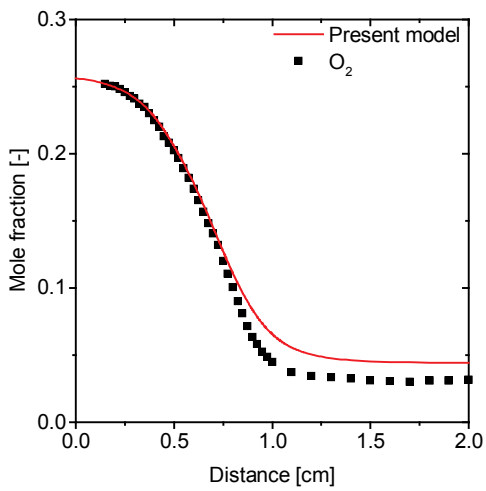

Figure 4. Examples from Paper III showing experimental and simulated species profile for oxygen from a burner stabilized flame.

3.2.5 The laminar burning velocity: method and simulations

The laminar burning velocity can provide information of the global reactivity regarding a fuel and oxidizer mixture [28]. As such, it plays an important role in the

development and validation of kinetic models. The definition of the laminar burning velocity and experimental techniques available for studying it are discussed in Chapter 4.

Simulations were carried out using the premixed laminar flame speed calculator in Chemkin. A grid independent solution was ensured. Transport properties are important when simulating flames and to provide a more accurate solution, the computationally demanding multicomponent transport option is often used. Thermal diffusion is another important parameter implemented in simulations of the laminar burning velocity, resulting in fewer radicals diffusing into the cold region. In the present study, thermal diffusion and multicomponent transport were taken into account in all the simulations that were performed.

3.2.6 Sensitivity

Sensitivity analysis is a useful tool for modelling development, providing an indication of which reactions that are of greatest importance for the given result of a specific model. The sensitivity can be defined as in (9).

$$s_i = \frac{\partial ln Y_k}{\partial ln \alpha_i} = \frac{\alpha_i}{Y_k} \frac{\delta Y_k}{\delta \alpha_i} \tag{9}$$

For reaction rate sensitivity, α_i represents the pre-exponential factor A in the Arrhenius expression, and Y_k the specific parameter of interest, such as the laminar burning velocity or species concentration. A reaction associated with a high degree of sensitivity indicates that the solution will be more strongly affected by changes in its rate constant, compared to reactions with a low sensitivity. Figure 5 presents a typical sensitivity figure of the laminar burning velocity at stoichiometric conditions for a methanol+air flame. In this example, the $H+O_2=O+OH$ and $HCO+M=H+CO+M$ are the most sensitive reactions.

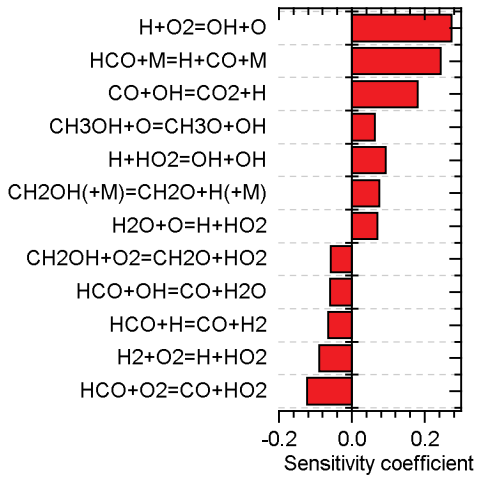

Figure 5. Sensitivity figure of the laminar burning velocity at 343 K and 1 atm for a methanol + air flame at stoichiometric conditions.

3.2.7 Modelling development process

Modeling development can be a laborious task which usually requires a vast amount of data from literature to be reviewed and evaluated. The mechanism developed for methanol and formaldehyde, as reported in Paper III, and later extended to the combustion of acetic acid, Paper IV, used version 0.6 of the Konnov mechanism [29] as a starting point. Prior to carrying out these studies, the base mechanism of hydrogen and syngas (H_2/CO) were reviewed [30, 31] in a manner similar to that described below. The reactions included in these two subsets are not discussed in Papers III or IV.

The modelling development undertaken in the thesis followed a protocol to create a structure for the rather vast process involved. First, mechanisms from the literature for the fuel of interest were studied. This led to a detailed review being made of all elementary reactions involved in the fuel specific subset. Reactions that were not included in the Konnov mechanism [29], but found to be of importance were added. The next step was to investigate the rate constants associated with each reaction.

Critical reviews of rate constants are an important tool for mechanism development. The work by Baulch et al. [32] is one of the most renowned ones, reviewing experimental data for several hundred reactions up till early in the 2000. Another important database is NIST.gov, which deals with data up to the year 2013. After reviewing the information provided by NIST.gov and Baulch et al. [32] for each of the reactions, all the literature published after the studies just cited was

considered. Information regarding the Arrhenius expression (Equation (3)) was collected. The choice of rate constant was based on the review of the literature, taking the quality of experiments and calculations, agreement between studies, and possible sources of errors into account. Rate constant expressions valid over a broad temperature range and based on experimental data were preferred.

Sometimes the rate constants found in the literature were not provided in the simple Arrhenius expression or were presented in a more complex way such as a two Arrhenius expressions. Problems of this sort were addressed in the following way. When data was available in tabulated form as a function of temperature, the Arrhenius expression was fitted using MATLAB [33]. If instead the rate constant was only provided as a complex expression the rate constants were first calculated in the specified temperature range and the Arrhenius expression was fitted to the data that was obtained.

All the reactions in the mechanism are reversible. The direction of the reaction implemented in the mechanism was selected based on which direction had the most reliable data available. For third body reactions, the information required for the Troe formula, see Equations (7) and (8), was implemented and as certain species have enhanced collisional efficiencies, these were included in the mechanism as well.

A total of 83 reactions altogether were reviewed for the methanol and formaldehyde subset and an additional 70 reactions were included to extend the mechanism to the combustion of acetic acid. A common practice in this field is to tweak the reaction constants within their experimental uncertainty limit to fit a particular dataset, creating a so-called optimized mechanism. This was not done for the mechanisms presented here. It allows the mechanism to more easily be updated in the future when more reliable data is available.

The thesis work covers several aspects of modelling development that are highlighted with red in Figure 6. In this work emphasis was placed on rate constants and reactions. No evaluation was performed with regards to thermodynamic data or transport properties. Accurate thermodynamic data was obtained from the database of A. Burcat currently administered by E. Goos [34]. The transport data used in this model are identical to the Konnov mechanism version 0.6 except for updates of the hydrogen subset as presented in [30]. The developed mechanism was validated using new experimental data of the laminar burning velocity as well as experimental results from the literature.

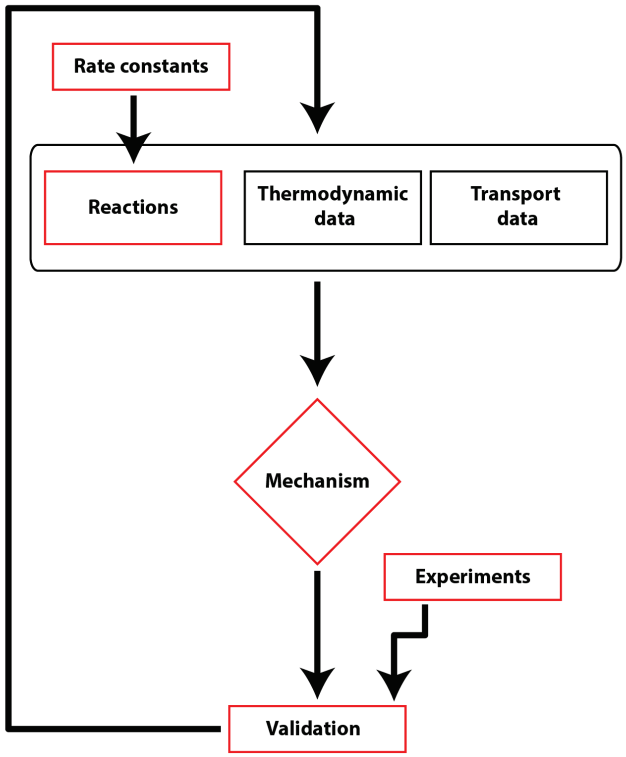

Figure 6. Flow chart of modelling development highlighting the work in this thesis in red.

4 The laminar burning velocity

The laminar burning velocity can be defined as the velocity at which a freely laminar flame propagates relative to the unburned gas. This parameter is important in combustion studies since it is a fundamental property of a combustible mixture, making it ideal for validating models. Experimental determination of it is hampered however, by the difficulty of generating a stationary, planar, freely propagating and adiabatic flame. Today, mainly three methods for measuring the laminar burning velocity exist.

4.1 Heat flux method

As an detailed review of the heat flux method was published recently by Alekseev et al. [35] only a brief account of the method and of certain details which are of importance to the thesis will be presented here.

4.1.1 Principle of the heat flux method

A schematic of the heat flux burner and a top view of a burner plate are shown in Figure 7. The burner generates a premixed stretch-free flat flame, ideal for determination of the laminar burning velocity. The burner can be divided into a cold and a hot part, separated by a ceramic ring for insulation purposes [36, 37]. The plenum chamber, belonging to the low-temperature part, is used to produce a uniform flow and to heat the unburned gas to the desired initial temperatures. The experimental studies resulting in the thesis were all performed at initial gas temperatures of 298-358 K.

To be able to measure the laminar burning velocity, the flame needs to be adiabatic. When it is stabilized on a burner however the flame loses heat to the burner plate resulting in a non-adiabatic situation. The heat flux burner was designed to circumvent this problem through heating the burner plate to a temperature above that of the unburned gas. As the gas passes the burner, it becomes heated, compensating for the heat loss of the flame. The burner plate is typically heated to

368 K. The temperature of the hot and the cold parts of the burner are controlled by two separate water baths.

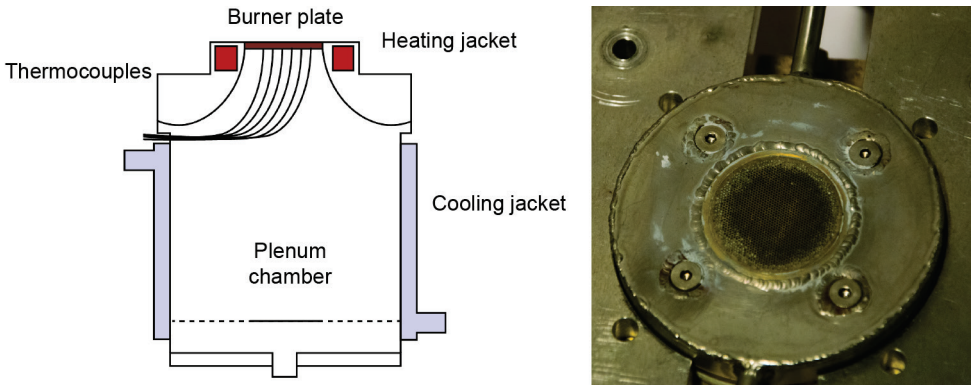

Figure 7. (left) Schematic of the heat flux burner, (right) A photograph of the burner plate used for the acetic acid experiments.

The laminar burning velocity is determined by varying the unburned gas velocity while simultaneously measuring the temperature of the burner plate. The temperature of the burner plate is affected by the distance of the flame from the plate which in turn is dependent upon the velocity of the unburned gas and the laminar burning velocity. Under experimental conditions, when the velocity of the unburned gas is lower than the laminar burning velocity, the flame is positioned close to the burner plate, the plate receiving more heat from the flame than it loses to the unburned gas. During conditions opposite to this, the flame is positioned further away, the burner plate then losing more heat to the unburned gas than it receives from the flame. The heat gain and heat loss of the burner plate result in a parabolic radial temperature profile that can be measured using thermocouples inserted into the burner plate. The temperature profile can be described by (10)

$$T(r) = T_{r=0} + Cr^2 \tag{10}$$

In the equation, $T_{r=0}$ is the temperature at the center of the burner plate, C is the polynomial coefficient and r is the radial placement of the thermocouples. An adiabatic state is found when the temperature profile is flat, i.e. when the C coefficient is equal to zero. Under these conditions, the net heat gain and heat loss is equal. In practice, the unburned gas velocity is set to levels above and below the laminar burning velocity, and the temperature profile is registered. The C coefficient

is then plotted as a function of the unburned gas velocity, the velocity at which C equals zero being determined by interpolation. The velocity corresponding to C=0 is then the laminar burning velocity. Examples of measured and fitted temperature profiles and of the plot of C versus the unburned gas velocity are shown in Figure 8. The slope of the linear fit is denoted sensitivity and is used for error analysis.

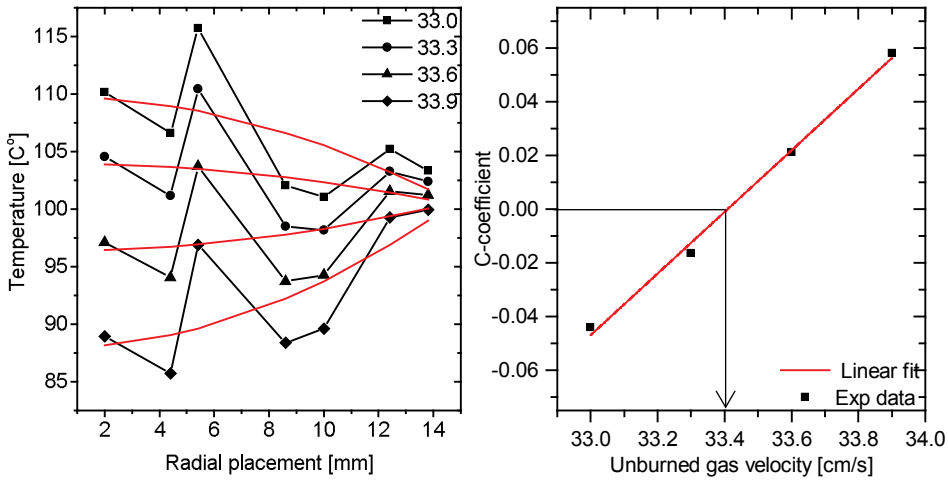

Figure 8. (left) Measured temperature profiles and fitted temperature profile, (right) Unburned gas velocity as a function of the C-coefficient. The laminar burning velocity is found at C(0)=33.4 cm/s.

Measurements can only be performed when the flame is flat. However, under certain experimental conditions cellular structures are formed in the flame. This process is rather complex and is due to hydrodynamic and diffusive-thermal effects [38]. The diffusive-thermal effect is caused by an imbalance in the heat and mass diffusivity and the hydrodynamic effect results in deflection of the streamlines causing high and low velocity regions. The laminar burning velocity was determined by extrapolation during these conditions. Usually the extrapolation distance (the difference between the highest unburned gas velocity and the laminar burning velocity) is less than 2 cm/s.

4.1.2 Heat flux setup

Experimental data was obtained using two heat flux setups, each equipped with an evaporator, the two evaporators being of different size. Setup I employs an evaporator with a smaller capacity than setup II, making it suitable for fuels of heavier molecular weight requiring smaller flows. It is important to select an evaporator of appropriate

size in order to maintain a stable flow of liquid and reduce the uncertainty. A photograph of Setup I is shown in Figure 9.

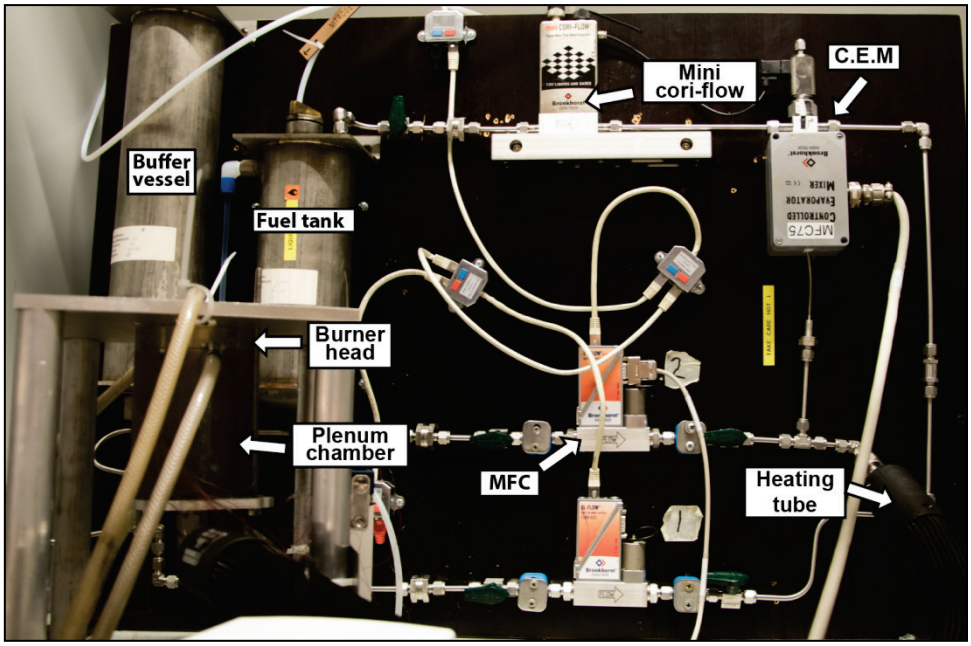

Figure 9. A photograph of Setup I showing the different components.

The desired composition of the mixture is achieved through use of a mixing panel controlled by use of LabVIEW script [35]. Gases are supplied from the central supply line of the laboratory and are controlled by use of mass flow controllers (MFCs). Buffer vessels are installed upstream of the MFCs to reduce possible fluctuations in the flow. Metering, transportation and evaporation of the liquid fuel are achieved using a mini cori-flow and a controlled evaporator and mixer (CEM). A carrier gas (air) is used to stimulate evaporation and to transport the vapor. All of the mass flow controllers and evaporators are from Bronkhorst High Tech.

Before being transported to the burner, the fuel and the oxidizer from the CEM are mixed with the remainder of the oxidizer to obtain the correct composition of the mixture. Since liquid fuels are used here, a heating tube is installed between the CEM and the burner. This is set to the same temperature as the plenum chamber so as to prevent condensation of the fuel. The vapor pressure of the fuel limits the amount of evaporated fuel that can be present in the total gas mixture; any surplus fuel condenses. For calculating the maximum equivalence ratio achievable, use is made of Equation (1), rewritten as Equation (11).

$$\phi_{max} = \left(\frac{O_2}{fuel}\right)_{st} \frac{\frac{P_f}{P}}{m_{O2}\left(1 - \frac{P_f}{P}\right)} \quad (11)$$

In this equation, the amount of fuel is expressed in terms of partial pressure, using the partial pressure rule $x_f=P_f/P$ where x_f is the mole fraction of the fuel, P_f the partial pressure of the fuel and P the total pressure of the gas mixture, set to atmospheric pressure. In order to calculate the maximum equivalence ratio which is attainable, the partial pressure of the fuel is set to its vapor pressure. The mole fraction of O_2 (m_{O2}) in the supply air is 21%. Here, the denominator of the second term accounts for the O_2 in the total mixture.

Calibration of the MFCs was performed by use of a piston meter (Bios DryCal Tech.) prior to the experimental procedures. The calibration curves, of third or fourth polynomial order, are inserted into the LabVIEW script, which corrects the flow set point accordingly.

The thermocouples that are inserted into the burner plate are of type T, E or N, and the signal being registered by use of a 16 channel thermocouple input module, National instruments 9213.

4.1.3 Uncertainties

The laminar burning velocities presented in Chapter 5 and 6 are displayed by both vertical and horizontal error bars. The vertical errors bars in the figures are based largely on the uncertainties that arise from the mass flow controllers, calibration and the temperature scatter.

The accuracy of the gaseous flow is evaluated using the error of the MFCs, which according to the manufacturer can be expressed as ΔU=0.5% (*reading*) + 0.1% (*full scale*), where *reading* is the actual flow through the MFC and *full scale* is the maximum flow. In a similar way, the accuracy of the liquid flow can be estimated using the uncertainty of the mini cori-flow; ΔU=0.2% (*reading*) + 0.5 g/h. One should avoid experimental conditions that results in flows close to the lower operational limits of the MFC (10% of full scale, as specified by the manufacturer), since this decreases the accuracy of the MFCs. The piston meter used for the calibration of the MFCs has a standardized flow accuracy of 1% of reading.

The uncertainties of the temperature scattering and the impact of the interpolation or extrapolation performed to determine the laminar burning velocity are both related to the temperature profile, as described by Equation (10). The effect

of temperature scatter on the laminar burning velocity can be estimated in the following way. The least square fit method is used to fit the measured temperature profile to the parabolic dependence of (10). By taking the standard deviation of the polynomial fit and dividing this by the slope of the interpolation performed when determining the laminar burning velocity, the uncertainty of the temperature scatter is determined.

The interpolation, index I, or extrapolation, index E, performed to derive the laminar burning velocity also creates uncertainty in the results. This is calculated by first determining the uncertainty of the parabolic coefficient when the unburned gas velocity equals the laminar burning velocity, as described in (12). To obtain the error in the laminar burning velocity this uncertainty is divided by the sensitivity. In Equation (12), S is the sum of square deviations between measured and fitted C values divided by the minimum points, n-2, required to make the fit as described by Eq. (13). Where $t_{\alpha/2}$ is the critical value of the t-distribution at 95% confidence level, C_i is the measured parabolic coefficient, a and b are fit parameters of the linear regression and $\overline{U_g}$ is the mean value of the unburned gas velocity. Usually the uncertainty can be sorted in decreasing order as TC-scatter, MFCs and extrapolation/interpolation. Typically the uncertainty of the interpolation and extrapolation is one order of magnitude smaller than the uncertainty from the flow and from the temperature scatter.

$$e_{I,E} = t_{\frac{\alpha}{2},n-2}\, S \sqrt{\frac{1}{n} + \frac{n\left(U_g^2 - \overline{U_g}\right)^2}{n\sum U_{g,i}^2 - \left(\sum U_{g,i}\right)^2}} \tag{12}$$

$$S = \sqrt{\frac{\sum\left(C_i - aU_{g,i} - b\right)^2}{n-2}} \tag{13}$$

The total uncertainty is then derived by adding the errors from the flows, the temperature scatter and the extrapolation and interpolation. The overall accuracy is typically better than ±1 cm/s.

The horizontal error bars in the laminar burning velocity figures represent the uncertainty of the equivalence ratios which are obtained from the standard accuracies of the MFCs and of the piston meter used for their calibration.

4.2 Stretched flame methods

Although the heat flux method is a simple technique for determining the laminar burning velocity, the method has certain limitations for high pressure and temperature. Two other methods are available for measurements of these types: the spherical flame method and the stagnation flame method.

4.2.1 Spherical flame method

Spherical flames are frequently used to measure the laminar burning velocity at elevated pressures [39, 40]. The fuel and oxidizer mixture is inserted into a closed chamber and is ignited centrally by use of electrodes. The laminar burning velocity can be obtained from the spherical flame in different ways. One simple approach is to register the radius of the propagating flame as a function of time, R(t), using an optical method. From R(t), the stretched flame speed, S_u, can be derived using the relation $S_u=dR/dt$. Stretch correction is then employed to correct for stretch, using either a linear or a nonlinear technique. Finally, the laminar burning velocity is obtained from the stretch-free flame speed using the density correction $S_L=S_u(\rho_b/\rho_u)$. In this expression ρ is the density of the burned, b, and unburned, u, densities at equilibrium.

The spherical flame method is subject to uncertainties, several of which are discussed in [40]. Some of the main challenges are those of radiation losses, instabilities of the flame and error in the equivalence ratio. It has been shown that use of linear and use of nonlinear extrapolation can differ in the results obtained for the laminar burning velocity. Despite these uncertainties, use of the spherical flame method is important for the combustion community, enabling high pressure flames to be investigated. Methane flames have been investigated for example at pressures of 60 atm [41].

4.2.2 Stagnation flame method

Stagnation flames are used to measure the laminar burning velocity both at higher pressures and temperatures than those present under ambient conditions. The method can be also be used to measure the extinction strain rate [42], which is a fundamental property used for model validation [43, 44]. The stagnation flame method [40, 45] is based on creating a stagnation plane e.g. through having two identical counter-flowing streams of fuel and oxidizer impinging upon one another. Upon ignition, two flames are established, one on each side of the plane as depicted

in Figure 10 (left panel). The flames cannot be used for determining the laminar burning velocity directly, since they are subjected to stretch. Stretch correction can be achieved by measuring the velocity profile of the axial velocity as a function of the distance from the nozzle for each of several different initial velocities. A typical axial velocity profile is shown in Figure 10 (right panel). The velocity measurements are typically performed using particle image velocity, PIV, or laser Doppler velocimetry, LDV. From each velocity profile, two parameters are derived: the reference speed, $S_{u,ref}$ and the impinging stretch, K. Plotting $S_{u,ref}$ as a function of K for each velocity profile extrapolation to zero stretch, using linear or nonlinear techniques, results in the stretch free reference speed, defined as the laminar burning velocity.

Many of the uncertainties of the method are discussed in [40]. For stagnation flames, nonlinear and linear extrapolation techniques differ from one another in the laminar burning velocities obtained, an effect mainly seen for fuels with heavy molecular weight. Additional uncertainties stem from the velocity measurements of the axial profile obtained by use of laser based methods. It is thus important to minimize the uncertainties of the seeding, laser alignment and alike.

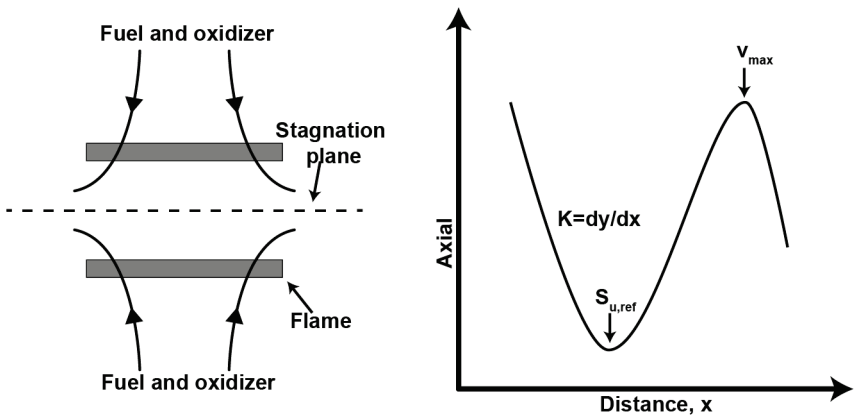

Figure 10. (left) A schematic showing the principle behind the stagnation flame method as outlined in the text. (right) The axial velocity as a function of nozzle distance.

4.3 Temperature dependence

Measuring the laminar burning velocity at standard conditions of 298 K and atmospheric pressure is important for model validation. Real life combustion however, often occurs at high pressure and temperature conditions. This can cause problems since such conditions can be challenging to achieve in laboratory

environments. Correlations are thus used frequently for predicting laminar burning velocities outside the experimentally available range of temperatures or pressures. The temperature dependence of the laminar burning velocity can be described by equation (14). In the expression S_{L0} is the laminar burning velocity at a reference temperature, T_0 is usually set to 298 K and alpha is the power exponent. Since the alpha coefficient can thus be used to derive the laminar burning velocity at higher temperatures, it is important to quantify it accurately. From here on the term *temperature-dependence* will be taken to mean the alpha coefficient.

$$S_L = S_{L0}\left(\frac{T}{T_0}\right)^{\alpha} \tag{14}$$

To derive the alpha coefficient, the laminar burning velocity is first plotted on a log-log scale as a function of temperature, as shown in Figure 11 (left panel). If the data is consistent, it follows from Equation (14) that the velocities for each equivalence ratio should follow a linear trend. Linear regression is then used to fit the data and the slope of the linear regression is the alpha coefficient. The alpha coefficient is presented in Figure 11 (right panel) as a function of equivalence ratio. As can be seen, the coefficient follows a parabolic behavior with a minimum at slightly rich mixtures. This indicates that the laminar burning velocity increases with a smaller rate with increasing temperatures than in the case of very rich or lean flames.

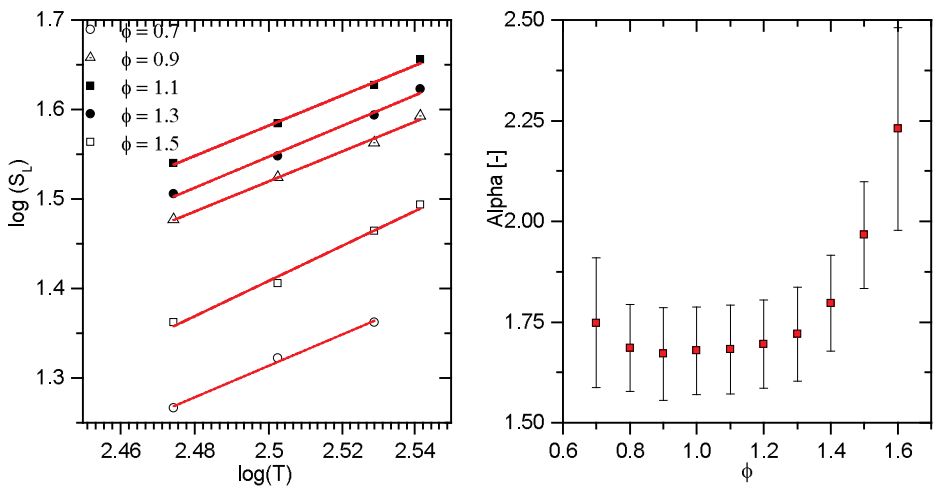

Figure 11. (left) Typical log-log plot of the laminar burning velocities of methyl formate + air as a function of initial gas temperature for odd values of ϕ. Symbols: experimental data and lines: linear fit of the measurements. (right) Power exponent, α, as a function of ϕ

The error bars of the alpha coefficient are dependent upon the uncertainty of each laminar burning velocity, ΔS_{Li}, as well as upon the uncertainty of the fit in Figure 11 (left panel). The error is calculated using Equation (15). To calculate the parameter $\Delta\alpha(S_{Li})$ of the expression the following steps are performed. First, temporary alpha coefficients, αi, are calculated by changing each experimental laminar burning velocity point, S_{Li}, to its uncertainty limit, $S_{Li}\pm\Delta S_{Li}$ and generating a linear fit for these new points. The slope of the fit is the coefficient αi. In order to estimate the contribution of the uncertainties in the laminar burning velocity, the original alpha coefficient, α_0, is subtracted from each temporary α_i, which then yields $\Delta\alpha(S_{Li})$.

$$\Delta\alpha = \sqrt{\sum_i \left[\Delta\alpha(S_{L,i})\right]^2} \tag{15}$$

5 Experimental data for model validation

In this chapter experimental data concerning the laminar burning velocity are presented and compared with calculated results using mechanisms from the literature, in addition, the temperature dependence of the laminar burning velocity is investigated both experimentally and numerically. The results are from Paper I and II and concern acetaldehyde (CH_3CHO) and methyl formate (CH_3OCHO).

5.1 Introduction

In order to develop a mechanism which is both accurate and reliable, it needs to be validated by experimental data obtained under a wide range of different conditions. Although many fuels have been investigated comprehensively, yielding a large set of useful data, there are some fuels and intermediates for which information concerning their combustion is scarce, unreliable or non-existent. Acetaldehyde a common intermediate formed during combustion of ethanol is one example of this. Although both the pyrolysis and oxidation of it has been investigated extensively [46], an accurate determination of its laminar burning velocity has not been reported earlier.

Another species of interest is methyl formate; an ester investigated earlier in terms of a wide range of properties under different conditions. Its laminar burning velocity has been reported in two earlier studies [47, 48], yet discrepancies between results of the two datasets were noted for particularly rich flames, creating problems for model validation.

A large part of the work that resulted in the thesis concerned measurements of the laminar burning velocities of fuels for which the data reported in the literature was inadequate, due to either too few experiments or none at all having been carried out. All the experiments were performed using the heat flux method, described in Chapter 4.

5.2 Laminar burning velocity of acetaldehyde

In Paper I, the laminar burning velocity of acetaldehyde + air was measured at atmospheric pressure and at initial gas temperatures of 298-358 K. The equivalence ratio was varied between 0.6 and 1.8. Figure 12 presents results obtained at 298 K, along with results reported by Gibbs and Calcote [49]. The latter results were obtained using the Bunsen burner technique, which produces stretched flames (as was discussed in connection with the stagnation and spherical flame methods in Chapter 4). However, since no stretch correction was applied in the work Gibbs' and Calcote's reported, their experimental data cannot be regarded as reliable. The measurements in the present study appear to be the first reliable data on this matter published. As can be seen in the figure, a comparison of the two sets of data shows them to be shifted relative to one another as the maximum velocity occurs at different equivalence ratios.

The experimental data obtained were compared with simulated results using three mechanisms from the literature, all of which can be used for ethanol combustion, those of Leplat et al. [50], Saxena and Williams [51], and Konnov [29]. Since acetaldehyde is a key species in ethanol combustion, the models should be able to reproduce the experimental result. As can be seen in Figure 12, the maximum velocity calculated for each of the mechanisms agrees rather closely with the new experimental result obtained here. The Leplat et al. mechanism shows the closest agreement of all between the calculated and the experimental data. This is not surprising, since the subsets of acetaldehyde and ethanol were revised in 2011.

A close look at Figure 12 shows that the Leplat et al. mechanism overpredicts the experimental results for lean and stoichiometric flames and underpredicts those obtained under rich conditions. To investigate which reactions affect the laminar burning velocity of the acetaldehyde flame, sensitivity analysis of the mechanism was performed. It is well known that the laminar burning velocity of hydrocarbon flames is governed mainly by the chemistry of the base subsets of H_2 and syngas and is often not particularly sensitive to fuel specific reactions. This is in line with the present observations, indicating greatest sensitivity to reactions from these subsets. Many of the sensitive reactions have rate constants originating from the optimized GRI 3.0 mechanism [52]. Interestingly enough, a similar pattern has been observed for the GRI 3.0 mechanism in simulating the laminar burning velocity of CH_4 flames [53]. This suggests that the behavior of the GRI mechanism was inherited, so to speak, by the Leplat mechanism, demonstrating the importance of having accurate C_1 and H_2/O_2 subsets.

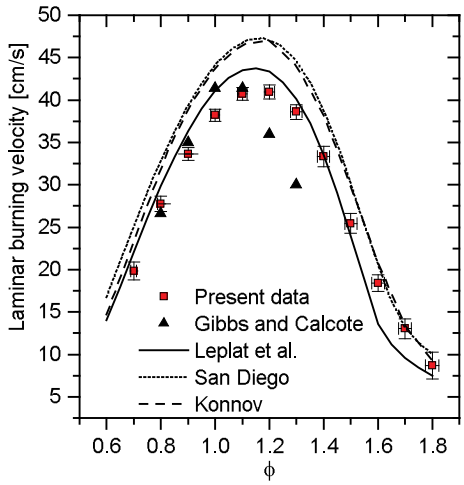

Figure 12. Laminar burning velocities of acetaldehyde and air at room temperature and 1 atm. Symbols: experiments, lines: modeling. Red squares: present data; Black triangles: data from [49]. Solid line, dashed line and dash-dot line: predictions of the mechanisms of Leplat et al. [50], Saxena and Williams [51], and Konnov [29], respectively.

5.3 Laminar burning velocity of methyl formate

In the study reported in Paper II the laminar burning velocity of methyl formate + air was measured at atmospheric pressure and at initial gas temperatures of 298-348 .K The equivalence ratio was varied between 0.7 and 1.6. The experimental data obtained were used to evaluate results reported earlier by Dooley et al. [47] and by Wang et al. [48] that showed various discrepancies in the case of rich flames. These earlier results had been obtained by use of the spherical and of the stagnation flame method respectively.

Figure 13 presents laminar burning velocities obtained here at 298 K. The results are compared with those reported by Dooley et al. [47] and by Wang et al. [48]. Overall a close agreement with the results of Wang et al. is evident. Both datasets show the maximum velocity to be at equivalence ratio of 1.1. The present results agree well with those reported by Dooley et al. for lean and slightly rich mixtures. For richer flames the laminar burning velocities of Dooley et al. are higher than those obtained in present study and in that of Wang et al.

The experimental results obtained here were also compared with simulations using mechanisms from the literature by Glaude et al. [54], Dievart et al. [55] and Dooley et al. [47] respectively. The first of these three mechanisms was derived for dimethyl carbonate but contains a subset for methyl formate, the latter two mechanisms were

derived for methyl formate combustion. The simulated results for each of these three mechanisms are included in Figure 13. It can be seen in the figure that none of the mechanisms predict the maximum velocity to occur at the same equivalence ratio of 1.1 as observed in the experimental study. The mechanism of Glaude et al. clearly overpredicts the present experimental results. In contrast, under lean and stoichiometric conditions, there is a close agreement of the results with predictions by both the Dievart and the Dooley mechanisms. For equivalence ratios above 1.1 these mechanisms overpredict the new experimental results obtained. The mechanisms for these rich flames are in better agreement with the data of Dooley et al. [47]. This is not surprising since the two mechanisms each contain the same subset in the case of methyl formate, one that stems from Dooley et al. [47]. The authors developed the kinetic mechanism by use of literature data as well as estimating values by investigating the hydrogen bond and reactivity of similar compound. The mechanism was slightly modified to be in closer agreement with the results obtained in their experimental study. This demonstrates the "risks" of modifying a mechanism to make it agree as closely as possible with a particular set of experimental data. The data of Dooley et al. obtained from spherical flames, was derived using a linear extrapolation technique which can possibly explain the deviation of the results from the present study and Wang et al. [48].

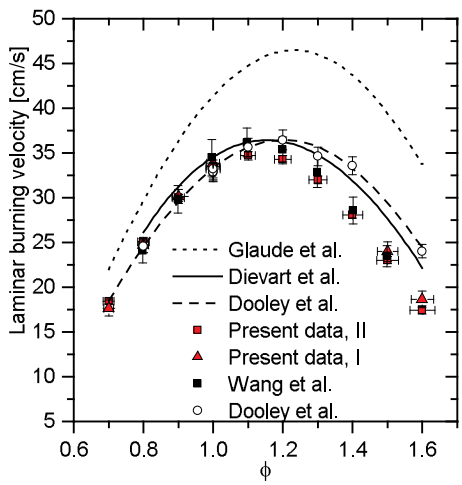

Figure 13. Laminar burning velocities of methyl formate + air as a function of ϕ at room temperature. Symbols: experimental data and lines: modelling. Red squares: results using heat flux setup I; red triangles: results using heat flux setup II; black squares: data from Wang et al. [48]; circles: data from Dooley et al. [47] ; solid line: Dievart et al. [55]; dashed line: Dooley et al. [47], dotted line: Glaude et al. [54].

5.4 Temperature dependence

The temperature dependence of the laminar burning velocity was investigated in studies of acetaldehyde and methyl formate, see Equation (14). This has been an approach commonly taken in various recent publications to validating kinetic models (see e.g. [56]). It was discovered however, as reported in Paper II, that, although the experimental and numerical alpha coefficients can be used for checking data consistency, they should not be used as a tool for validating mechanisms. To demonstrate that this is the case, the alpha coefficients of methyl formate, derived as discussed in Chapter 4, are presented in Figure 14. The experimental data obtained is compared with the results of modelling using the mechanisms of Glaude et al. [54] and Dievart et al. [55]. As it can be seen, the two mechanisms are very similar in their temperature dependence. This is surprising, since the two mechanisms predict very different laminar burning velocities, as can be seen in Figure 13. The calculated alpha coefficients are seen to be in close agreement with the experimental data under at lean and slightly rich conditions. To investigate the reactions responsible for the temperature dependence, so as to obtain a better understanding of the chemistry involved, sensitivity analysis was used.

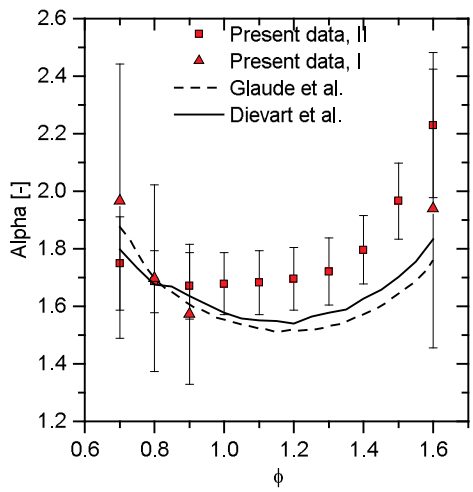

Figure 14. Power exponent, α, as a function of ϕ. Symbols: experimental data and lines: modelling. Squares: results obtained using heat flux setup II, triangles: results obtained using heat flux setup I; Dashed line: Glaude et al. [54], solid line: Dievart et al. [55]

5.4.1 Alpha sensitivity

A sensitivity analysis of the alpha coefficient appears to not have been performed earlier, and unlike sensitivity analysis of the laminar burning velocity it cannot be conducted directly by use of the chemical kinetic software. An expression for the alpha sensitivity was derived, which includes the sensitivity of the laminar burning velocity at two different temperatures. The expression is based on the definition of the sensitivity presented in Chapter 3, but specified here for the laminar burning velocity as shown in (16)

$$Sens(S_L, k) = \frac{\partial S_L}{\partial k}\frac{k}{S_L} \tag{16}$$

In a similar way, the sensitivity of the alpha coefficient as a function of the rate constant can be defined as in (17)

$$Sens(a, k) = \frac{\partial a}{\partial k}\frac{k}{a} \tag{17}$$

The fact that the sensitivity of the laminar burning velocity and of the alpha coefficient are both functions of k and that the temperature dependence can be described by Equation (14), enables the partial derivatives with respect to k to be calculated using the product rule. The normalized sensitivity of the alpha coefficient with respect to k can then be described as in (18)

$$Sens(a, k) = \frac{Sens\left(S_{L,T}, k\right) - Sens(S_{L,T0}, k)}{ln\left(\frac{T}{T_0}\right)a} \tag{18}$$

In this equation $Sens(S_{L,T},k)$ is the sensitivity of the laminar burning velocity at an elevated temperature, set here to 398 K, and $Sens(S_{L,T0},k)$ is the sensitivity at a reference temperature of 298 K. Since the sensitivity analysis were performed under stoichiometric conditions, the alpha coefficient in the equation above, represents the values it has at 1.0 in Figure 14.

5.4.2 Sensitivity results

The sensitivity of both the laminar burning velocity and of the alpha coefficient is shown in Figure 15. Sensitivity analysis of the laminar burning velocity was performed using the mechanisms of Glaude et al. [54] and Dievart et al. [55] at 298 and 398 K and used in Equation (18) to derive the sensitivity of alpha. If the sensitivity of the laminar burning velocity increases with increasing temperature, i.e. if the sensitivity is greater at 398 K than at 298 K, the sensitivity of the alpha coefficient is displayed with a positive sign. If the sensitivity of the laminar burning velocity instead decreases with increasing temperature, i.e. if the sensitivity is greater at 298 than at 398 K, the alpha sensitivity will have a negative sign. If the sensitivity at 298 K and at 398 K is roughly equal, the sensitivity of the alpha coefficient will be small and thus insignificant. A reaction displayed in the figure with a high degree of sensitivity means that the two temperatures differ considerably in the sensitivity, i.e. the reaction is temperature dependent.

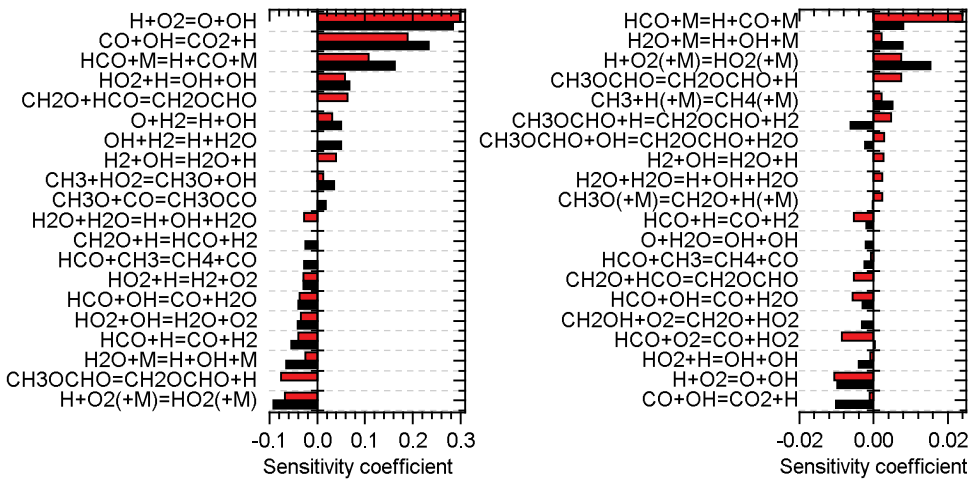

Figure 15. Sensitivity of the Glaude et al. [54] and Dievart et al. [55] mechanisms. (left) Sensitivity of the laminar burning velocity at 298 K, (right) Sensitivity of the power exponent.

One thing that can be clearly observed in Figure 15 is that the sensitivity of the alpha coefficient is approximately one order of magnitude smaller than that of the laminar burning velocity. Despite the differences in magnitude, the two panels in Figure 15 show the strongest sensitivity overall to the same reactions: $CO+OH=CO_2+H$ (R1), $H+O_2=O+OH$ (R2), $HO_2+H=OH+OH$ (R3), $HCO+M=H+CO+M$ (R4) and $H+O_2(+M)=HO_2(+M)$ (R5). It is important to note that the sign of these reactions changes where in Figure 15 (left panel) R1, R2, R3 and R4 are all chain branching reactions and are thus displayed with positive

sensitivity, whereas in Figure 15 (right panel) these reactions have a negative sign associated with them, indicating that the sensitivity of the reactions is smaller at 398 K than at 298 K. The same can be seen for the chain inhibiting reaction of R5, in which the sign switches from negative to positive.

In comparing the two panels, it can also be seen that the sensitivity of the laminar burning velocity of both mechanisms is very similar in terms of reactions and magnitude. For the alpha sensitivity however, there are many reactions that only one of the mechanisms shows sensitivity to. One can likewise note that some of the reactions appears to have a sensitivity that increases with temperature for the one mechanism, but decreases for the other, resulting in a reaction with both positive and negative signs such in the case of the $CH_3OCHO+H=CH_2OCHO+H_2$ reaction. Finally it can be observed that many of the reactions is the alpha sensitivity are fuel specific.

The above discussion shows that the sensitivity of the alpha coefficient can provide a different view on the chemistry involved, providing information of reactions importance with increasing/ decreasing temperature. As the sensitivity of alpha is roughly 1 order of magnitude smaller than the laminar burning velocity, a change in rate constant generating a 20% difference in the laminar burning velocity will result in a 2% change in alpha. This explains why mechanisms that cannot reproduce the experimental laminar burning velocities can still be in good agreement with the experimental alpha coefficients. Seeing that two mechanisms can predict the laminar burning velocity so differently yet have very similar temperature dependence, clearly demonstrate that direct comparison between experiments and modelling should not be used to validate the mechanism. Yet, direct comparison can be useful to identify large experimental deviations and to evaluate data consistency as deviations between experiments and modeling most probably indicates problems in the measurements.

6 A new mechanism for small oxygenated fuels

In this chapter selected results of the oxygenated fuel mechanism performance, that were presented in Papers III and IV are shown and discussed. Important reactions from the reviewed subsets will be highlighted. Note that the subset of methanol and formaldehyde will from here on be referred to as the "*C_1 subset*", and that reactions in the smaller subsets of H_2 and syngas [30, 31] will not be discussed. Since the mechanism was first developed for methanol and formaldehyde (Paper III) and later was extended to acetic acid (Paper IV), the chapter will first present the results of the sub mechanism of methanol and formaldehyde, this being followed by the results of acetic acid.

6.1 Methanol and formaldehyde

Methanol is the simplest alcohol molecule and as such is a key species in the combustion of larger hydrocarbons. Another matter of importance is that methanol is oxidized to carbon dioxide via formaldehyde which is a toxic pollutant. It is important to understand the formation and consumption of formaldehyde and, together with this, the combustion of methanol, in order to be able to reduce formaldehyde emission. Efforts of this sort, together with the increased use of methanol as a transportation fuel, have resulted in the development over the years of several detailed mechanisms for methanol combustion. The first comprehensive methanol combustion mechanism was developed by Westbrook and Dryer [57] in 1979. The mechanism was able to successfully reproduce flow reactor and shock tube experiments carried out under a wide range of conditions. As new kinetic and thermochemistry data became available, the Dryer group published two more mechanisms [58, 59] in the two decades that followed. These studies eventually resulted in the renowned methanol model of Li et al. [60] in 2007. The mechanism was validated extensively for carbon monoxide, formaldehyde and methanol combustion experiments, and an overall good agreement was observed for a wide range of data. Metcalfe et al. have since then developed the Aramco mechanism

version 1.3 [61], considered today to be one of the best contemporary models available for the combustion of smaller hydrocarbons and oxygenated fuels. The base H_2/CO mechanism includes the optimized syngas subset of Kéromnès et al. [62].

The goal of Paper III was to develop a contemporary mechanism for the combustion of methanol and formaldehyde using unmodified rate constants from the literature, following the procedure outlined in Chapter 3. This resulted in a mechanism which may not be ideal but can be used as a starting point for an optimized mechanism, appropriate for a specific set of experiments.

The mechanism was validated against a wide range of experimental data resulting in just over 40 validation runs. Overall, the temperature was varied between 300 and 1960 K and pressure was varied from 0.03 to 100 atm. The experiments included species profiles of oxidation and pyrolysis in shock tubes and flow reactors, burner stabilized and freely propagating flames, as well as ignition delay times. The validation runs presented below represent different combustion scenarios that demonstrate the overall performance of the mechanism. Results of the new mechanism are compared with simulations using Aramco, since this is currently considered to be most reliable model for small oxygenated fuels.

6.1.2 Validation of formaldehyde

In this section, simulated results using the new mechanism will be compared with experimental data on the combustion of formaldehyde. The mechanism will first be compared with results of a shock tube experiment followed by flow reactor data and finally with flames. These experimental conditions cover a wide range of temperatures, from 300 to 1805 K, and pressures from 0.03 to 6 atm.

Figure 16 (left panel) presents normalized formaldehyde profiles during formaldehyde pyrolysis in a shock tube. Experimental data [63] and simulations were performed with initial conditions of 2.81 atm and 1805 K. The present mechanism shows close agreement with the experimental result while the Aramco mechanism [61] predicts the decomposition of formaldehyde to occur faster than it was experimentally measured. To obtain insight into which reactions the concentration of formaldehyde, sensitivity analysis was performed.

Results of the sensitivity analysis are shown in Figure 16 (right panel). As can be seen, the formaldehyde concentration is dependent upon reactions involving HCO, such as $HCO+H=CO+H_2$ and $HCO+M=H+CO+M$. From the new C_1 subset, the highest level of sensitivity can be seen to the reactions of $CH_2O+H=HCO+H_2$, $CH_2O+M=HCO+H+M$ and $CH_2OH+HCO=CH_2O+CH_2O$. These reactions are discussed briefly in section 6.1.3.

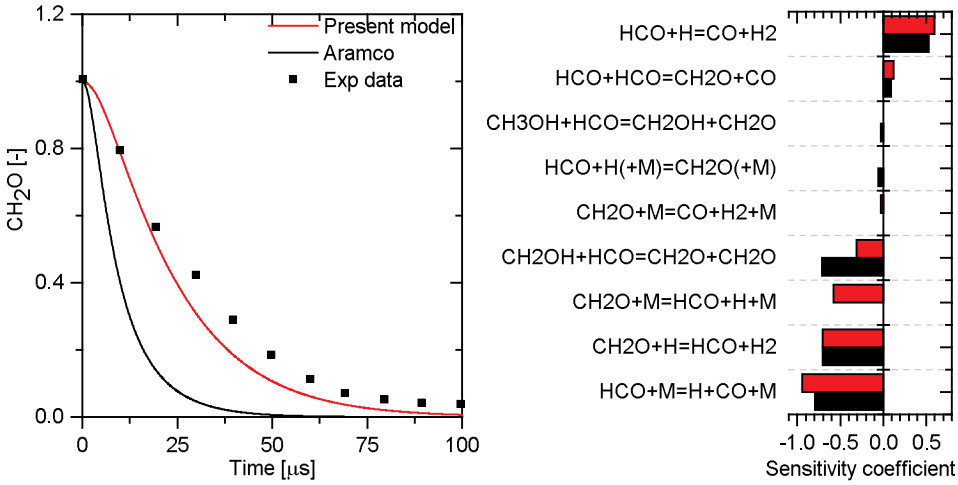

Figure 16. (left) Shock tube formaldehyde profiles of formaldehyde pyrolysis. Initial conditions are CH_2O=4%, Ar=96% at 2.81 atm and 1805 K. Lines are modelling predictions and symbols experimental data from [63]. (right) Reaction rate sensitivity of formaldehyde. The sensitivity was evaluated at the time corresponding to the normalized value of 0.25 in the left figure.

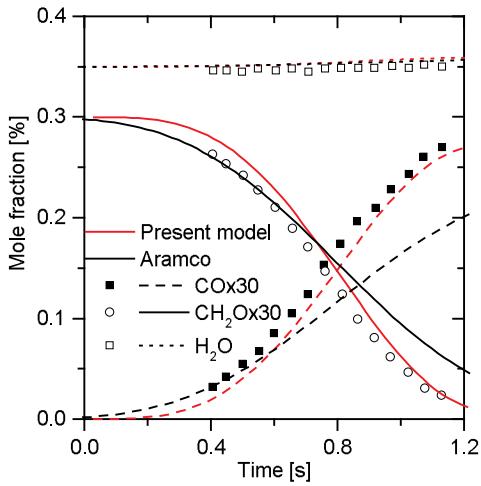

Figure 17. Flow reactor species profiles of formaldehyde oxidation. Initial conditions are: CH_2O=100ppm, O_2=1.5%, H_2O=0.35%, N_2=98.14% at 6 atm and 852 K. Lines are modelling predictions and symbols experimental data from [60]. Modelling was shifted to 50% of experimental formaldehyde consumption.

Figure 17 presents experimental data and simulations of formaldehyde oxidation in a flow reactor. Experimental data [60] and simulations were performed with initial conditions of 6 atm and 852 K. The new mechanism was able to successfully

reproduce the experimental results. The Aramco mechanism [61] is in close agreement with the experimental data of formaldehyde and H_2O as well, yet it underpredicts the formation of CO after 0.7 s.

The two examples above demonstrate that the new mechanism was able to reproduce data at elevated pressures and temperatures. The next two figures present experimental data of flames stabilized at atmospheric pressure and below.

The laminar burning velocity of 1,3,5-trioxane ($C_3H_6O_3$) was measured experimentally [64] and simulated at 373 K and 1 atm, as shown in Figure 18 (left panel). Under experimental conditions, 1,3,5-trioxane decomposes rapidly into three formaldehyde molecules and the flame properties being considered to be associated almost entirely with chemistry of formaldehyde [64]. The fuel loading was set to 5%, the O_2 mole fractions, $O_2/(O_2+N_2+\text{fuel})$, being varied during the experiments.

In order to simulate the experimental results, the subset of 1,3,5-trioxane provided by the Santner et al. [64] was included in both the present and the Aramco mechanism. Both mechanisms are in close agreement with the results at low O_2 ratios. The two mechanisms predict a decline in the laminar burning velocity with an increasing ratio; this is not being observed however, in the experimental results. For higher O_2 concentrations the present mechanism underpredicts the experimental result, while the Aramco mechanism is in close agreement with the data.

A sensitivity analysis of the laminar burning velocity of 1,3,5-trioxane that was performed is shown in Figure 18 (right panel). Greatest sensitivity can be seen for the chain branching reactions of $H+O_2=OH+O$, $CO+OH=CO_2+H$ and $HCO+M=H+CO+M$. Such chain inhibiting reactions as $HCO+O_2=CO+HO_2$ and $H+O_2(+M)=HO_2(+M)$ are also important. From the recently updated C_1 subset, only the reaction of $CH_2O+H=HCO+H_2$ appears in the figure.

Species profiles of a low-pressure burner stabilized formaldehyde flame are presented in Figure 19. The experimental results [65] and simulations were performed at 30 mbar. Both mechanisms are in close agreement with the experimental data. There is a slight shift between the simulations of the two mechanisms, since the Aramco mechanism predicts production of species to start at lower heights above the burner.

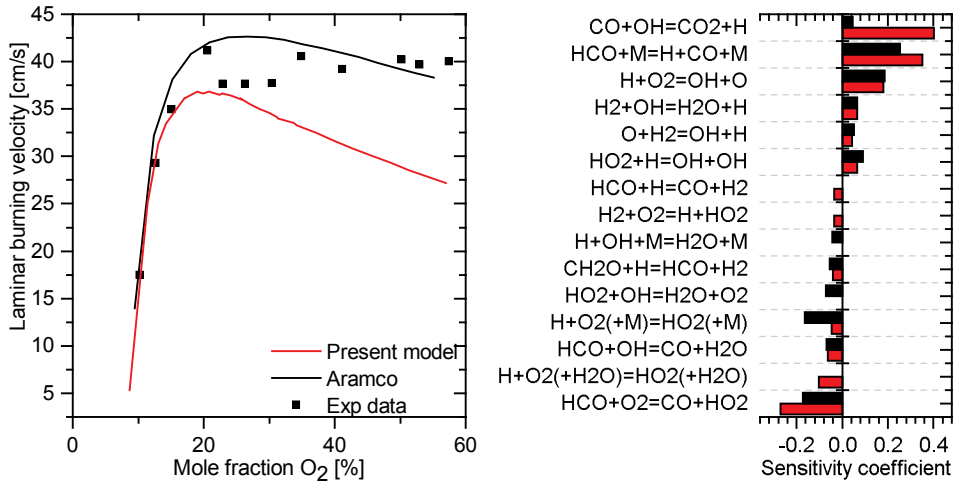

Figure 18. (left) Laminar burning velocity of 1,3,5-trioxane at 1 atm and 373 K. Fuel loading was fixed to 5 molar % with varying $O_2/(O_2+N_2+fuel)$ ratio. Lines are modelling predictions and symbols experimental data from [64]. (right) Flow rate sensitivity analysis of 1,3,5-trioxane+O_2+N_2 laminar burning velocity. The analysis was performed at 1 atm and 373 K and O_2 mole fraction of 0.25.

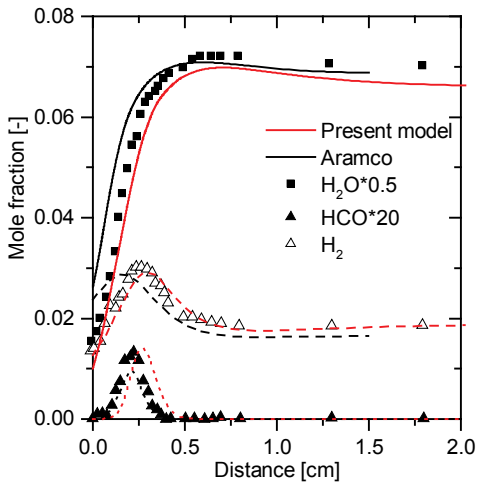

Figure 19. Species profiles of a formaldehyde flame. Initial conditions are: CH_2O=17.7%, O_2=16.3%, Ar=66.0% at 30 mbar. Lines are modelling predictions and symbols experimental data from [65].

6.1.3 Important reactions of formaldehyde combustion

The sensitivity analysis presented in section 6.1.2 can be used to obtain a better understanding of why the results of the present mechanism and of the Aramco

mechanism are different. The reactions identified to be of importance to formaldehyde combustion are discussed below. The numbering of the reactions used here is the same as in Paper III, so as to facilitate direct comparison. For a more detailed discussion regarding the choice of the rate constants the reader is directed to Paper III.

R2. $CH_2O+H=HCO+H_2$

During radical rich hydrocarbon combustion, formaldehyde is consumed mainly through hydrogen abstraction by H, OH, O or CH_3. Abstraction by the hydrogen atom often dominates [66]. In Paper III, R2 was seen in many of the sensitivity figures, indicating the reaction to be important under a wide range of conditions in connection to formaldehyde combustion. In the present mechanism the rate constant of Wang et al. [66] was accepted, since it is in close agreement with several experimental datasets and it covers a wide range of temperatures. In the Aramco mechanism an expression of Baulch et al. [32] is used.

R3. $CH_2O+M=HCO+H+M$

The decomposition of CH_2O has two product channels: $CH_2O+M=HCO+H+M$ and $CH_2O+M=CO+H_2+M$. R3 is an important reaction in the combustion of formaldehyde, since it is chain branching generating both primary and secondary hydrogen atoms [67]. In the present mechanism, the rate constant of R3 originates from a theoretical study by Troe [68]. This expression was based on experimental data and covers a wide range of temperatures. In the Aramco mechanism [61], R3 is incorporated in the reverse direction the rate constant used there originating from Laskin et al. [69]

R4. $CH_2OH+HCO=CH_2O+CH_2O$

The reaction of $CH_2OH+HCO$ has two product channels: $CH_2OH+HCO=CH_2O+CH_2O$ (R4) and $CH_2OH+HCO=CH_3OH+CO$. It has previously been demonstrated that the reverse reaction of R4 is important for CH_2O pyrolysis, especially at high concentrations of CH_2O (1.5-3.7%) [70]. In the present mechanism, the rate expression for R4 of Li et al. [60] was accepted. This rate constant is based on experimental data obtained by Friedrichs et al. [70]. In the Aramco mechanism the rate constant of Tsang et al. [71] was used.

R6. $CH_2O+HO_2=HCO+H_2O_2$

It has been observed previously that R6 is important to include in the oxidation mechanism of formaldehyde [63]. In the present mechanism the rate expression of Baulch et al. [32] was accepted for R6. In the Aramco mechanism an expression

theoretically derived by Li et al. [72] was used. The two expressions are in generally close agreement.

R8. $CH_2O+O_2=HCO+HO_2$

This reaction has been shown to be of importance in hydrocarbon combustion [73, 74]. It has been investigated both experimentally and theoretically and the agreement between the various studies involved being close. For the present mechanism, the rate constant of Baulch et al. [32] was selected, since it is in good agreement with recent theoretical and experimental results. In the Aramco mechanism the experimental rate of Srinivasan et al. [74] was used.

6.1.4 Validation of methanol

In this section, simulated results using the new mechanism are compared with methanol combustion experiments. First, results of the mechanism are compared to ignition delay times, followed by comparison with flow and perfectly stirred reactor data and finally by comparison with the laminar burning velocity. The experimental conditions cover a wide range of temperatures, from 300 to 1330 K, and pressures from 1 to 20 atm.

Shock tube ignition delay times at 10 atm and 1330-1050 K are shown in Figure 20 (left panel). The ignition delay time was defined experimentally as the time between the shock reflection from the end wall and the intercept of the maximum derivative of the CH-radical emission curve with initial signal level. Since excited CH is not included in the present mechanism, the ignition delay time used for the simulations was defined as the time corresponding to the maximum OH concentration. This instant matches the maximum production of the ground state CH in the simulations. Both mechanisms predict longer ignition delay times than those measured experimentally. To investigate which reactions that influence the ignition delay time, a sensitivity analysis was performed at 1180 K. The result is seen Figure 20 (right panel). The highest degree of sensitivity from the updated C_1 subset is that of the $CH_3OH+HO_2=CH_2OH+H_2O_2$ reaction. This is closely followed by the reactions of $CH_3OH+O_2=CH_2OH+HO_2$, $CH_2O+HO_2=HCO+H_2O_2$ and $CH_3OH+H=CH_2OH+H_2$. From the hydrogen subset, the $H_2O_2(+M)=2OH(+M)$ and $2OH=H_2O_2+O_2$ reactions are important.

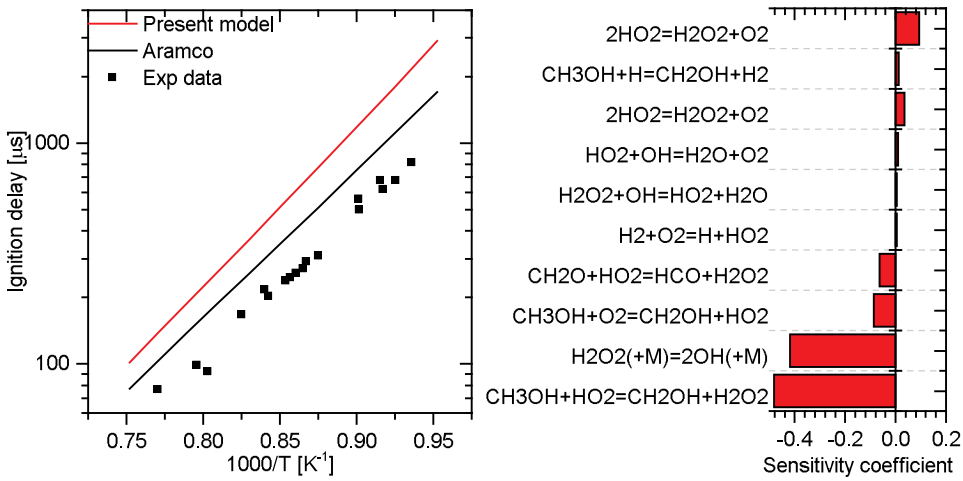

Figure 20. (left) Shock tube ignition delay times as a function of temperature. Initial conditions: CH_3OH=5.7%, O_2=8.6%, Ar=85.7% at 10 atm and 1330-1050 K. Lines are modelling predictions and symbols experimental data from [75]. (right) Reaction rate sensitivity of ignition delay time. The sensitivity was performed at 1180 K with the same mixture and pressure as in the left hand figure.

Species profiles measured during methanol oxidation in a flow reactor at 20 bar are presented in Figure 21. The two mechanisms are in close agreement overall with the experimental data of methanol. For the species profiles of O_2 and CO the Aramco mechanism predicts consumption and production to occur at lower temperatures than those observed experimentally. The present mechanism is in better agreement with CO and O_2.

Species profiles measured during methanol oxidation in a perfectly stirred reactor at 10 atm are shown in Figure 22 (left panel). The present model is in close agreement with the experimental profiles of CH_3OH, CO and H_2O. The Aramco mechanism predicts the consumption of CH_3OH and the onset of H_2O production to occur at lower temperatures than those measured experimentally. Both mechanisms fail to reproduce the CO_2 profile, as the simulated results are lower than the experimental data. To obtain insight into the reactions responsible for the CO_2 concentration, a sensitivity analysis was performed and is presented in Figure 22 (right panel). Although the highest level of sensitivity was found of the updated C_1 subset to the $CH_3OH+O_2=CH_2OH+HO_2$ reaction, an overall sensitivity to reactions from the H_2 and syngas subsets could be observed.

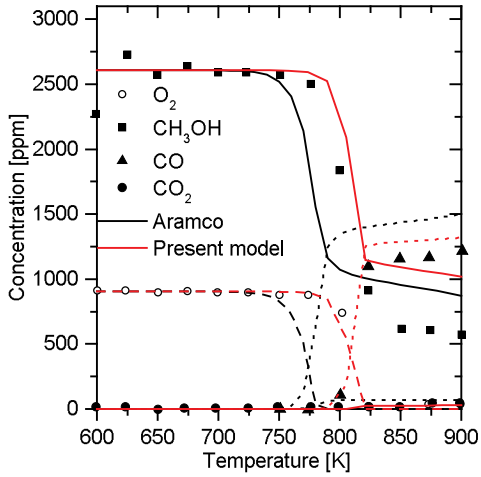

Figure 21. Flow reactor species profiles of CH_3OH oxidation. Initial conditions are: CH_3OH=2606 ppm, O_2=904 ppm at 20 bar and 600-900 K. The mixture was diluted with N_2. Residence time was set to 1317/T. Lines are modelling predictions and symbols experimental data from [76].

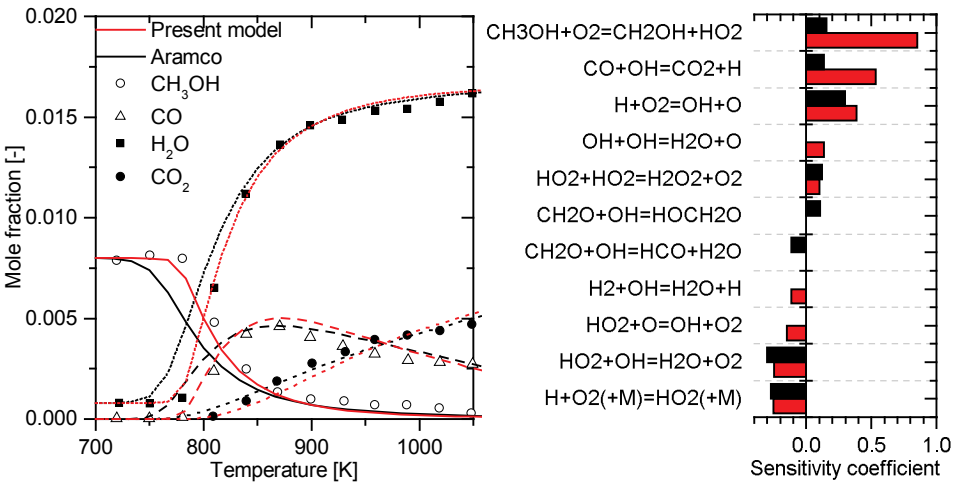

Figure 22. (left) PSR species profiles of CH_3OH oxidation. Initial conditions are: CH_3OH=8000 ppm O_2=20000 ppm, H_2O=800 ppm at 10 atm and 700-1100 K. The mixture was diluted with N_2. Residence time was set to 1 s. Lines are modelling predictions and symbols experimental data from [77]. (right) Reaction rate sensitivity of CO_2. The sensitivity was performed at 925 K with the same mixture and pressure as in the left hand figure. The sensitivity was evaluated at the time corresponding to the CO_2 mole fraction value of 3E-3 (left).

The laminar burning velocity of methanol under oxy fuel conditions (65% CO_2+35% O_2), measured at 1 atm and temperatures of 308 and 358 K is shown in Figure 23 (left panel). Both mechanisms were found to overpredict the laminar burning velocity under rich conditions. The maximum velocity of the two mechanisms is shifted to slightly richer flames than for the experimental data, resulting in a closer agreement under the lean conditions. The two mechanisms predict the same velocities for equivalence ratios higher than 1.4.

A sensitivity analysis of the laminar burning velocity, shown in Figure 23 (right panel), was performed at 308 K under stoichiometric conditions. The major sensitive reactions are the same as for the 1,3,5-trioxane flame, reactions from the H_2 and syngas subset demonstrating the importance of the base mechanisms. Note that version 0.6 of the Konnov mechanism, which was used as a starting point for the new mechanism, underpredicted the laminar burning velocity of methanol+air flames by approximately 15 cm/s at stoichiometric conditions. The new mechanism is in much better agreement for all of the methanol flames that were investigated.

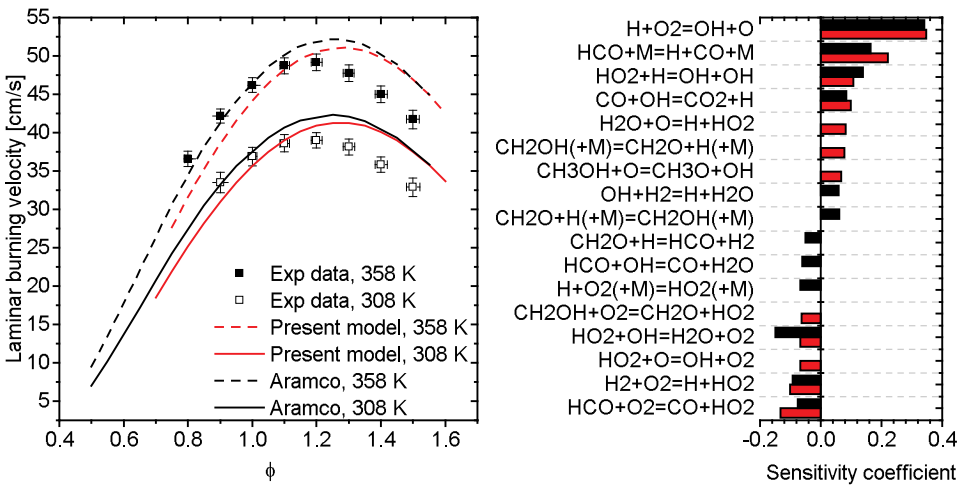

Figure 23. (left) The laminar burning velocity of methanol+oxy-fuel flames at 1 atm and 308-358 K. Lines are modelling predictions and symbols experimental data from [78]. (right) Flow rate sensitivity analysis of methanol+oxy-fuel laminar burning velocity. The sensitivity was performed at 1 atm, 308 K and ϕ = 1.0.

6.1.5 Important reactions of methanol combustion

On the basis of the sensitivity analysis reported in Paper III, the following reactions from the updated C_1 subset could be identified as being important for the combustion of methanol. The numbering of the reactions used here is the same as in Paper III, so as to facilitate direct comparison. For a more detailed discussion regarding choice of rate constants, the reader is directed to Paper III.

R15. $CH_3OH+H=CH_2OH+H_2$

The reaction of CH_3OH+H has two product channels: $CH_3OH+H=CH_2OH+H_2$ (R15) and $CH_3OH+H=CH_3O+H_2$. The hydrogen abstraction reactions by atomic hydrogen are one of the major consumption pathways for methanol [79, 80]. For the present mechanism, the rate constant expression of Peukert and Michael [80] was accepted for R15. This rate is in excellent agreement with the overall rate recommended by Baulch et al. [32]. The theoretical expression of Meana-Paneda [79] was used in the Aramco mechanism.

R16. $CH_3OH+HO_2=CH_2OH+H_2O_2$

The reaction of CH_3OH+HO_2 has two product channels: $CH_3OH+HO_2=CH_2OH+H_2O_2$ (R16) and $CH_3OH+HO_2=CH_3O+H_2O_2$. R16 is of importance for many different combustion properties [59, 60]. It is thus essential that this reaction is included in a CH_3OH reaction mechanism. Several theoretical studies have recently been published suggesting that R16 and not the second channel dominates. The rate constant of Alecu and Truhlar [81] was accepted for R16, since it shows a close agreement with other theoretical results as well as the only experimental study [82] available. In the Aramco mechanism, the authors use a different expression.

R17. $CH_3OH+O_2=CH_2OH+HO_2$

The reaction of CH_3OH+O_2 has been proposed to have three product channels; $CH_3OH+O_2=CH_2OH+HO_2$ (R17), $CH_3OH+O_2=CH_3O+HO_2$ and $CH_3OH+O_2=CH_2O+H_2O_2$. The channel generating CH_3O+HO_2, was suggested by Klippenstein et al. [83] and by Shayan and Vahedpour [84] to be insignificant. The reaction of methanol with molecular oxygen is important in methanol combustion [84], since the CH_2OH and HO_2 radicals can both decompose and generate additional hydrogen atoms. Despite this, R17 is not well understood. There are no experimental data available and the theoretical studies [83, 84] contradict each other. Based on the current state of knowledge of similar reactions, R17 have been accepted

to be the only product channel and was assigned the expression by Klippenstein et al. [83]. In the Aramco mechanism an expression of Walker [85] was used.

6.1.6 Discussion of methanol and formaldehyde subset

In Paper III, it was observed that the present mechanism was able to reproduce many CH_2O and CH_3OH experiments. Most importantly, the present mechanism showed a much closer agreement with the laminar burning velocity of methanol than version 0.6 of the Konnov mechanism. Still, the present mechanism was sometimes unable to reproduce the experimental results; one example is oxidation of very rich CH_2O mixtures in flow reactors. Another important matter is that the present mechanism and Aramco often produced similar results, demonstrating that the rate constants available are often of high quality. As more reliable rate constants are produced, the discrepancy between the simulated results of modified and of unmodified mechanisms will surely decrease.

6.2 Acetic acid

Acetic acid (CH_3CO_2H) is found in abundance in the environment [10] and studies have implied acetic acid to be formed by traffic: see e.g. [86, 87]. Nevertheless, relatively little information regarding the role of acetic acid in combustion is available. Zervas et al. have investigated the emissions of acetic acid from engines [88, 89] as well as burner stabilized flames of propane, isooctane and toluene/isooctane [90]. These studies have indicated emissions of acetic acid to be increased as the equivalence ratio decreases. To further investigate the formation of acetic acid, Battin-Leclerc et al. [91] developed a detailed kinetic mechanism. Simulated results were compared to experimental data from the propane flames by Zervas et al. [90] with an acceptable level of agreement. However the simulations failed to reproduce the experimentally observed increase of acetic acid emissions at leaner conditions. The mechanism of Battin-Leclerc et al. was not sufficiently validated due to the scarce amount of experimental data available.

More recently, Leplat and Vandooren [92] investigated species profiles of burner stabilized acetic acid flames, both experimentally and numerically. A detailed mechanism was developed based on a previous ethanol model by the same group [50] with additional reactions of importance to acetic acid. The mechanism was largely constructed using rate constants from the literature, yet some modifications and assumptions were made in order to improve the modelling results.

The goal of Paper IV was twofold. 1) To experimentally determine for the very first time the laminar burning velocities of acetic acid. 2) To extend the model of Paper III to the combustion of acetic acid using unmodified rate constants from the literature. The mechanism was validated against the new experimentally determined laminar burning velocities of acetic acid, as well as species profiles of a burner stabilized acetic acid flame [92].

6.2.1 Experiment

The laminar burning velocities of acetic acid were measured using two heat flux setups at initial gas temperatures of 338-358 K. The main challenge of measuring acetic acid on the present setup is the corrosiveness of the acid toward the brass burner. For this reason the burner with the worst characteristics (burner 1), as described in [35], was selected. The laminar burning velocity of the acetic acid was measured for three consecutive days, and the data being analyzed initially a discussed in Chapter 4. It was observed that the laminar burning velocity became lower each day. In order to translate the measured velocities into reliable data, the laminar burning velocities of methane at 298 K were employed. Two sets of data were required: the laminar burning velocity of methane measured each day on burner 1 prior to the acetic acid experiments, and the results for methane obtained using a reference burner. The reference burner was estimated to have a small uncertainty of less than ±0.5 cm/s. The laminar burning velocity of acetic acid was then calculated by use of (19)

$$S_{L,real} = \frac{S_{L,acid}}{S_{L\,CH4}} S_{L,CH4\,ref} \tag{19}$$

In the equation, $S_{L,acid}$ and $S_{L,CH4}$ are the measured velocities of acetic acid and methane, respectively using burner 1. $S_{L,CH4,ref}$ represent the laminar burning velocities obtained using the reference burner. The uncertainties of the new experimental results were estimated to be ±2 cm/s.

6.2.2 Validation of acetic acid subset

In this section, simulated results using the mechanism will be compared with acetic acid flames. The mechanism will first be compared with new experimental data

concerning the laminar burning velocity and then with species profiles of a burner stabilized flame.

The laminar burning velocities at 348 K are shown in Figure 24 (left panel). The measurements performed on three consecutive days, are in close agreement: all the discrepancies being within the error bars. The maximum velocity of the experimental results is found at stoichiometric conditions. The data is compared with modelling using the acetic acid mechanism presented in Paper IV. The simulated velocities are a few cm/s higher than the experimental results, and the maximum velocity is calculated at equivalence ratio 1.1. The mechanism overpredicted the experimental results at all temperatures investigated.

To identify reactions of importance for the laminar burning velocity of acetic acid, a sensitivity analysis was performed at 348 K and equivalence ratios 0.7, 1.0 and 1.3 as shown in Figure 24 (right panel). As can be seen for the laminar burning velocity of methanol and 1,3,5-trioxane flames, the main sensitive reactions belong to the H_2 and the syngas subsets. The remaining sensitive reactions, however, belong to the C_2 subset and involve reactions of ketene (CH_2CO) and of the ketenyl radical (HCCO). This suggests that discrepancies between the experimental data and the simulations are due to reactions of ketene and ketenyl radicals. Important reactions are $CH_2CO+OH=HCCO+H_2O$, $HCCO+O_2=CO_2+CO+H$, $CH_2CO+OH=CH_2OH+CO$ and $CH_2CO+H=CH_3+CO$.

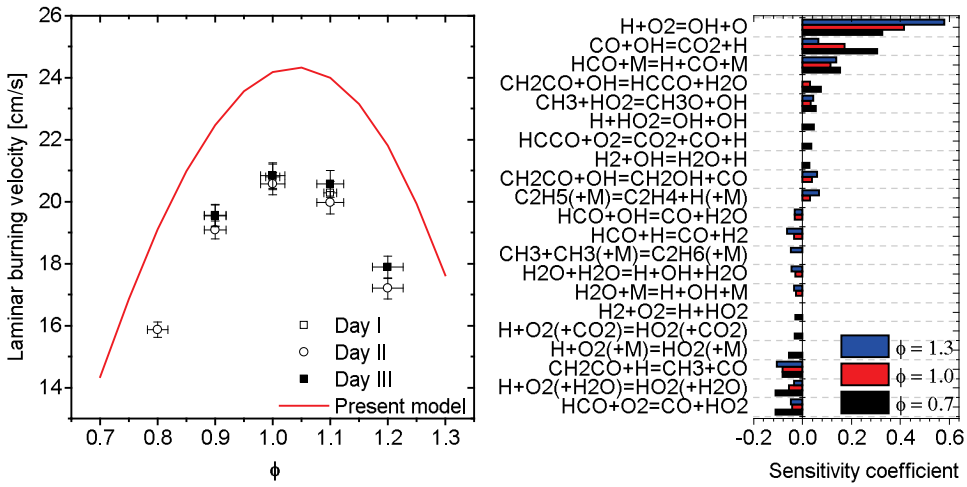

Figure 24. (left). Laminar burning velocities of acetic acid +air at 348 K. Lines are modelling predictions and symbols experimental data. (right) Flow rate sensitivity at 348 K and equivalence ratios 0.7, 1.0 and 1.3.

The simulations were also compared with burner stabilized flames, measured experimentally by Leplat et al. [92] at 50mbar and an equivalence ratio 0.9. While the new mechanism was able to successfully reproduce the major species, discrepancies were observed for minor intermediates as the mechanism either over-or-under predicted the experimental results. Shown in Figure 25 are selected species profiles.

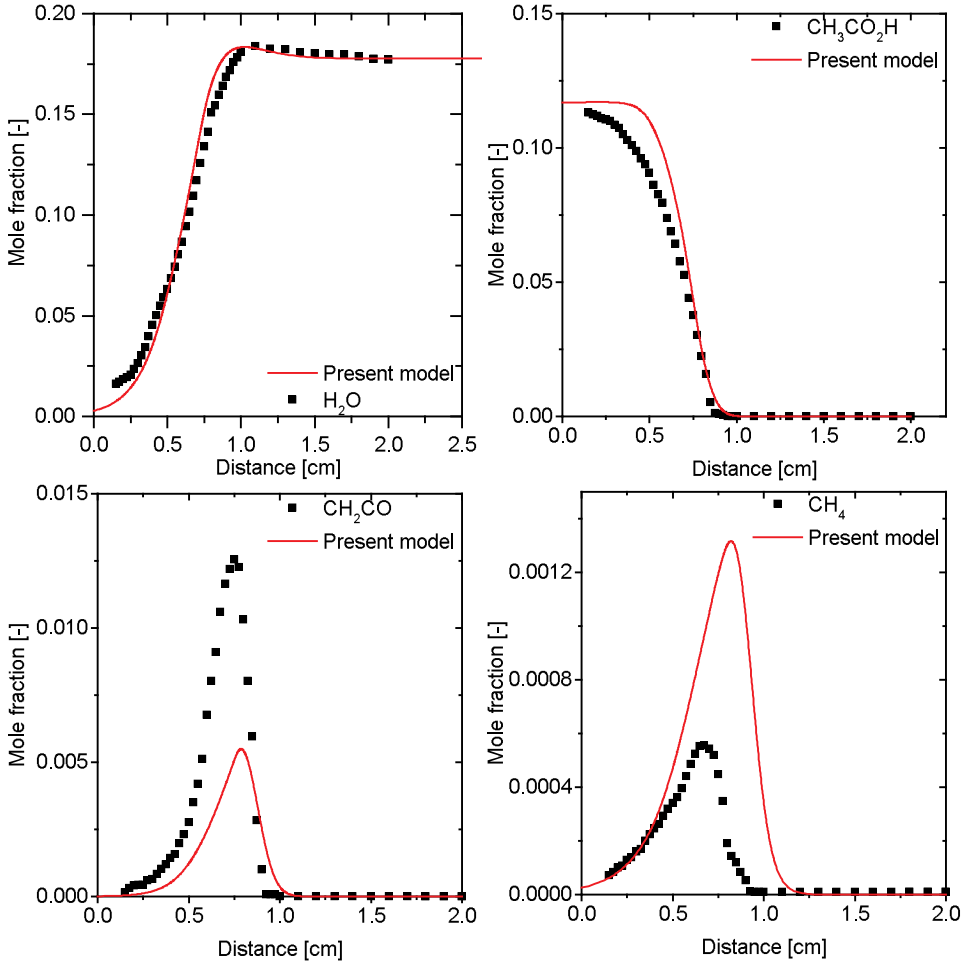

Figure 25. Species profiles of (top left) H_2O, (top right) CH_3CO_2H, (bottom left) CH_2CO, (bottom right) CH_4. Lines are modelling predictions and symbols experimental data from [92].

To gain further insight into why the mechanism is unable to reproduce the experimental results of the minor species, sensitivity analysis was performed. The results indicated ketene to play an important role for many of the species; this was also observed for the laminar burning velocity. A sensitivity analysis of ketene is shown in Figure 26. Several reactions of high sensitivity are ones involving CH_2CO_2H. The $CH_2CO_2H=CH_2CO+OH$ reaction is one of the main production

pathways for ketene. The reaction involving ketene which has the highest degree of sensitivity is the $CH_2CO+H=CH_3+CO$ reaction, which displays negative sensitivity as the reaction consumes ketene.

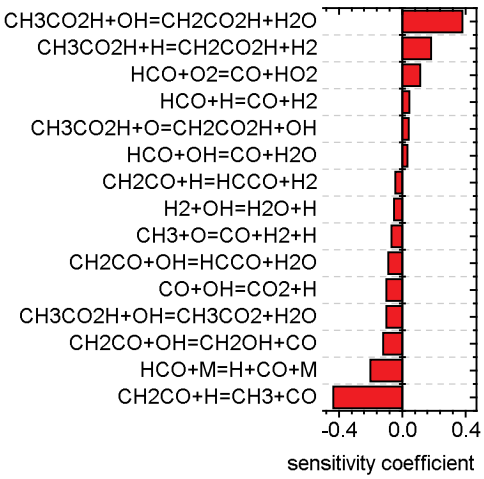

Figure 26. Sensitivity of CH_2CO.

6.2.3 Important reactions of acetic acid combustion

On the basis of the sensitivity analysis reported in Paper IV, the following ketene reactions from the reviewed acetic acid subset could be identified as being important for the laminar burning velocity and the species profiles of burner stabilized flames. The numbering of the reactions used here is the same as in Paper IV to facilitate direct comparisons. For a more detailed discussion regarding the choice of rate constant the reader is directed to Paper IV.

R10. $CH_2CO+OH=CH_2OH+CO$ and R11. $CH_2CO+OH=HCCO+H2O$

The reaction of CH_2CO+OH has several product channels: $CH_2CO+OH=CH_2OH+CO$ (R10), $CH_2CO+OH=HCCO+H2O$ (R11), $CH_2CO+OH=CH_2O+HCO$ and $CH_2CO+OH=CH_3+CO_2$. Reactions of CH_2CO with OH are important not only for combustion but also for atmospheric chemistry [93]. For the present mechanism, the overall temperature-independent rate constant of Baulch et al. [94] was adopted, together with the branching ratios calculated by Hou et al. [93].

R35. $HCCO+O_2=CO_2+CO+H$

The reaction of $HCCO+O_2$ has three products channels: $HCCO+O_2=CO_2+CO+H$ (R35), $HCCO+O_2=CO+CO+OH$ and $HCCO+O_2=O+CHOCO$. R35 increases the reactivity of the flame by producing hydrogen atoms. In the present mechanism, the theoretical rate constant of Klippenstein et al. [95] was adopted for R35, since the rate expressions were in close agreement with the overall experimental data of Carl et al. [96].

R2. $CH_2CO+H=CH_3+CO$

R2 is important for flame propagation as well as for the overall production of CH_3. The theoretical and experimental rate constants of this reaction are in reasonable agreement. In the present study the most recent rate constant of Senosiain et al. [97] was used.

R62. $CH_3CO_2H+OH=CH_2CO_2H+H_2O$

The reaction of CH_3CO_2H+OH has two product channels: $CH_3CO_2H+OH=CH_2CO_2H+H_2O$ (R62) and $CH_3CO_2H+OH=CH_3CO_2+H_2O$. This reaction is one of the major sinks of acetic acid in the atmosphere [98]. R62 is important for the concentration of ketene, since it is formed when the CH_2CO_2H radical decomposes. For the present mechanism, the accepted rate constant for R62 was based on a recent theoretical study of Mendes et al. [99] and on the experimental data of Khamaganov et al. [100]. The theoretical expression was found to deviate by a factor 2 from the experimental data and the rate constant expression of Mendes et al. was subsequently multiplied by 2.

R57. $CH_3CO_2H+H=CH_2CO_2H+H_2$

Similar to hydrogen abstraction by means of the OH radical, this reaction also produces CH_2CO_2H and this reaction is thus important for ketene. Limited rate constant data for this reaction led Leplat et al. to use the estimated value of Gasnot et al. [101]. The rate constant from the theoretical study of Mendes et al. is 4 times lower at 2000 K and 10 times lower at 500 K than the estimated value of Gasnot et al. The rate constant of Mendes et al. [99] was accepted in the present study.

R19. $CH_2CO+CH_3=C_2H_5+CO$

Although this reaction was not included in the sensitivity figures presented in Paper IV; it is an important reaction, since it defines the rate of C_2 formation [92]. The rate constant of this reaction is scattered, Hidaka et al. [102] suggested a value of 9E10 $cm^3mol^{-1}s^{-1}$ whereas Woods and Haynes [103] suggested the value of 5E12 $cm^3mol^{-1}s^{-1}$. When the value of Woods and Haynes was used, the mechanism was

found to be able to reproduce experimental C_2H_2 and C_2H_4 profiles. In the present mechanism the rate of Borisov et al. [104] was however accepted in the end since this was in close agreement with the rate constant of Hidaka in their temperature range (1100-1920 K).

6.2.4 Discussion of acetic acid subset

The mechanism described in Paper III was successfully extended in Paper IV to the combustion of acetic acid. Simulations were compared with new experimental data on the laminar burning velocity of acetic acid. It was observed that the calculated velocities overpredicted the experimental results by 3 cm/s. The mechanism was also compared with species profiles of a burner stabilized acetic acid flame. Although minor species were over or under predicted, close agreement with the major species could be noted. Sensitivity analyses performed for both the laminar burning velocity and the species indicated the importance of ketene in the combustion of acetic acid.

7 Concluding remarks

7.1 Summary

The two aims of this thesis were:

1) To measure the laminar burning velocity of fuels with limited or scattered data available, in order to extend the experimental database for kinetic mechanism validation.

2) To develop a contemporary detailed kinetic mechanism, for small oxygenated fuels and intermediates through use of unmodified rate constants obtained from the literature.

By fulfilling the first of these two aims, the thesis has provided the scientific community with new experimental data that can be highly useful for model validation. This is especially important for the combustion of acetaldehyde and acetic acid for which previously experimental results were unreliable or nonexistent respectively.

Regarding the second aim, a new mechanism for formaldehyde, methanol and acetic acid combustion was developed using unmodified rate constants from the literature. The mechanism was validated for a wide range of different conditions, with overall close agreement to several experimental results.

The work concerned with the first aim was reported in Papers I and II in which new experimental data of the laminar burning velocity was presented for acetaldehyde and methyl formate. The experimental results were compared to mechanisms from the literature. In Paper I, the laminar burning velocity of acetaldehyde was compared to simulations using three mechanisms. The best agreement between experimental data and modelling was found for a recently updated mechanism for acetaldehyde. Yet discrepancies were observed as the mechanism both over and under predicted the experimental results at lean and rich conditions. Using sensitivity analysis, it was indicated that the discrepancy between experiments and simulations originate from reactions of the sub-mechanisms of C_1 and H_2/O_2. In Paper II the laminar burning

velocity of methyl formate was compared with both experimental and numerical data. The paper investigated the temperature dependence of the laminar burning velocity as expressed by the relationship $S_L=S_{L0}(T/T0)^{\alpha}$. A sensitivity analysis of the alpha coefficient was performed for here the first time, the result providing insight into the temperature sensitive reactions involved.

The second aim was achieved in the work reported in Papers III and IV, in which a detailed kinetic mechanism for small oxygenated fuels was developed. The new mechanism was found to be in acceptable agreement to the experimental data. The subset of methanol and formaldehyde from Paper III were validated against experimental results from different combustion devices involving a wide range of different pressures, temperatures and species concentrations. The subset of acetic acid from Paper IV was compared with new experimental data of the laminar burning velocity of acetic acid, which was measured here for the first time. Experiments were performed at 338-358 K and at atmospheric pressure. The possible effects on the burner of the corrosiveness of the acid resulted in uncertainties of ±2 cm/s. It was observed that the mechanism overpredicted the experimental results by 3 cm/s. The model was compared to species profiles of burner stabilized flames with close agreement to major species. In view of the lack of kinetic information available, the sub mechanism was judged to be a success.

7.2 Outlook

In Paper III it was observed that the mechanism of Dooley et al. was not able to reproduce the experimental results of the laminar burning velocity for methyl formate. Therefore, our next step is to validate the mechanism for methyl formate combustion, adding our new experimental data to the database. In the same manner, the mechanism can be validated against the acetaldehyde results from Paper I, further expanding the mechanism.

Overall, the results reported in the thesis can be seen to be of value to the combustion community since they provided an in-depth analysis of a detailed kinetic mechanism for small oxygenated fuels and intermediates.

Acknowledgments

First of all I would first like to thank my supervisors Professor **Alexander Konnov** and Dr. **Elna Heimdal Nilsson**. During these years I have learned so much and the two of you have pushed me further than I thought was possible. I owe you my deepest thanks.

As no man is an island, neither is a PhD and there are so many that deserve my greatest gratitude. First I would like to thank **Per P.**, **Andreas E.** and **Christian B.** for being great discussion partners, you guys are my heroes! **Jenny** and **Vladimir**, the two of you have been such a great support, I could never have done this PhD without you. Sven-Inge you have been a great friend and confidant and I appreciate that you always have time for me.

I have made many friendships over the years, and while I cherish all of them, there are a few that I feel obliged to mention. **Emil N.** you certainly know how to enjoy life and I always have so much fun with you. **Karin M!** You have been such an amazingly good friend and you became even better when you found **Martin**. It is seldom that I find people who enjoy "5 O'Clock somewhere" as much as me, so you two are definitely keepers. **Nille** and **Malin J.**, the two of you have been great friends and I could never have survived these years without your love and support and just remember that it's never too late to get that tattoo... Just sayin'. **Jocke** you are too cool for school and you always make me smile, I am really appreciative for our friendship. **Fahed,** I feel like our friendship started of slow and is now kicking up a storm. I am intrigued to see where we land. **C.K.** (**Jesper**) it may sound corny but the one of the best time I've ever had in the lab was when we did our measurements. It was just great to hang out by ourselves. **Johan S.**, thank you for always being there to cheer me up and giving me good sci-fi advice.

Special thanks must also be given to Professor **Marcus Aldén, Minna, Cecilia** and **Igor** and of course the entire library staff of Sweden who provided me with rate constant articles at a constant rate. There are so many other people that have made each day at combustion physics fun and exciting. The lunch league: **Erdzan**, **Hesam**, and **Richard W, Anna-Lena, Joakim, Rasmus, Siyuan, Linda** and **Elias**. Arguments mixed with laughter, my cup of tea. **Kajsa, Elin, Dina** and **Giota,** while it may have come relatively late, your friendships have been a blessing. All of you have been a

great support as has everyone else at the Division of **Combustion Physics**. Of course, no research is complete without generous funding sources. In this case, this project could not have been possible without the financial support of the Swedish Research Council (VR) and Center for Combustion Science and Technology (CECOST).

Now, I know it may sound suspicious but I do have a few friends outside of Combustion Physics. **Liza** one does possibly not have a best friend above the age of 12 but you are mine! And I cannot tell you how glad I am that you accepted that chocolate bar all those years ago. A special thanks to **Lovisa B**. who gave me the courage to leave Gothenburg. **Sara M.**, It is great that we are still friends after living in different cities for so long; you have proven to be an exceptional friend, I could not be luckier to have you. **Friday** it was love at first sight, 'nuff said. **Ellen** and **Maria** I am so glad we could create our own league in Malmö. I want to give special thanks to **Henrik S.**, **Julia**, **Felix, Anna S., Jens, Rickard S.** and **Olivia** for being just normal fun drama free friends!! **Cassie** and **Gustav**, you are sorely missed!

I want to give a special thanks to Henrik's **family** for all the fun times. You guys have really made me feel at home in Skåne and I could not ask for a better extended family. I especially want to thank **Johan, Maria, Calle and Minna**, hanging out with you guys is one of my favorite things to do.

To my own family, words cannot express how highly I think you all. I am eternally grateful for **mum** and **dad** and that you supported me and let me do my own thing. My only regret about leaving Gothenburg is that I do not live close to my siblings, **Felic(z)ia, Joel, Lov**e and **Agnes**. You guys are the most amazing people and I feel so lucky that I have you in my life.

Last but not least, **Henrik**, You are Sam to my Dean, Phil to my Claire, Reagan to my Chris... simply put, my everything.

References

[1] C. K. Law, *Comprehensive description of chemistry in combustion modeling*. Combustion Science and Technology, vol. 177, pp. 845-870, 2005.

[2] C. K. Law, C. J. Sung, H. Wang and T. F. Lu, *Development of comprehensive detailed and reduced reaction mechanisms for combustion modeling*. Aiaa Journal, vol. 41, pp. 1629-1646, 2003.

[3] C. K. Westbrook and F. L. Dryer, *Chemical kinetic modeling of hydrocarbon combustion*. Progress in Energy and Combustion Science, vol. 10, pp. 1-57, 1984.

[4] E. Ranzi, A. Frassoldati, R. Grana, A. Cuoci, T. Faravelli, A. P. Kelley and C. K. Law, *Hierarchical and comparative kinetic modeling of laminar flame speeds of hydrocarbon and oxygenated fuels*. Progress in Energy and Combustion Science, vol. 38, pp. 468-501, 2012.

[5] T. Poinsot and D. Veynante, *Theoretical and Numerical Combustion (3rd ed)*. Bordeaux, France: Aquaprint, 2001.

[6] K. Kohse-Höinghaus, P. Oßwald, T. A. Cool, T. Kasper, N. Hansen, F. Qi, C. K. Westbrook and P. R. Westmoreland, *Biofuel Combustion Chemistry: From Ethanol to Biodiesel*. Angewandte Chemie International Edition, vol. 49, pp. 3572-3597, 2010.

[7] C. Arndt, R. Benfica, F. Tarp, J. Thurlow and R. Uaiene, *Biofuels, poverty, and growth: a computable general equilibrium analysis of Mozambique*. Environment and Development Economics, vol. 15, pp. 81-105, 2010.

[8] A. Månsson, A. Sanches-Pereira and S. Hermann, *Biofuels for road transport: Analysing evolving supply chains in Sweden from an energy security perspective*. Applied Energy, vol. 123, pp. 349-357, 2014.

[9] J. S. Gaffney and N. A. Marley, *The impacts of combustion emissions on air quality and climate - From coal to biofuels and beyond*. Atmospheric Environment, vol. 43, pp. 23-36, 2009.

[10] A. Chebbi and P. Carlier, *Carboxylic acids in the troposphere, occurrence, sources, and sinks: A review*. Atmospheric Environment, vol. 30, pp. 4233-4249, 1996.

[11] S. M. Sarathy, P. Oßwald, N. Hansen and K. Kohse-Höinghaus, *Alcohol combustion chemistry*. Progress in Energy and Combustion Science, vol. 44, pp. 40-102, 2014.

[12] X. Pang, Y. Mu, J. Yuan and H. He, *Carbonyls emission from ethanol-blended gasoline and biodiesel-ethanol-diesel used in engines*. Atmospheric Environment, vol. 42, pp. 1349-1358, 2008.

[13] J. Song, K. Cheenkachorn, J. Wang, J. Perez, A. L. Boehman, P. J. Young and F. J. Waller, *Effect of Oxygenated Fuel on Combustion and Emissions in a Light-Duty Turbo Diesel Engine*. Energy & Fuels, vol. 16, pp. 294-301, 2002.

[14] A. K. Agarwal, *Biofuels (alcohols and biodiesel) applications as fuels for internal combustion engines*. Progress in Energy and Combustion Science, vol. 33, pp. 233-271, 2007.

[15] M. Z. Jacobson, *Effects of ethanol (E85) versus gasoline vehicles on cancer and mortality in the United States*. Environmental Science & Technology, vol. 41, pp. 4150-4157, 2007.

[16] M. L. Bell, A. McDermott, S. L. Zeger, J. M. Samet and F. Dominici, *Ozone and short-term mortality in 95 us urban communities, 1987-2000*. JAMA, vol. 292, pp. 2372-2378, 2004.

[17] J. H. P. Seinfeld, S.N., *Atmospheric chemistry and physics: from air pollution to climate change*. Hoboken, New Jersey, John Wiley & Sons.

[18] F. A. Lindemann, S. Arrhenius, I. Langmuir, N. R. Dhar, J. Perrin and W. C. McC. Lewis, *Discussion on "the radiation theory of chemical action"*. Transactions of the Faraday Society, vol. 17, pp. 598-606 1922.

[19] H. H. Carstensen and A. M. Dean, *Comprehensive Chemical Kinetics* vol. 42, 2007.

[20] R. G. Gilbert, K. Luther and J. Troe, *Theory of thermal unimolecular reactions in the fall-off range .2. Weak collision rate constants*. Berichte Der Bunsen-Gesellschaft-Physical Chemistry Chemical Physics, vol. 87, pp. 169-177, 1983.

[21] CHEMKIN 10112, Reaction Design, San Diego, 2011.

[22] G. A.G. and I. R. Hurle, *The Shock Tube in High Temperature Chemical Physics*. London, England: Chapman & Hall Ltd., 1963.

[23] K. Kuo, *Principles of Combustion (2nd ed)*, John Wiley & Sons, 2005.

[24] Z. Zhao, M. Chaos, A. Kazakov and F. L. Dryer, *Thermal decomposition reaction and a comprehensive kinetic model of dimethyl ether*. International Journal of Chemical Kinetics, vol. 40, pp. 1-18, 2008.

[25] O. Herbinet and G. Dayma, Jet-Stirred Reactors, in *Cleaner Combustion*, F. Battin-Leclerc, J. M. Simmie, and E. Blurock, Eds., Springer, 2013.

[26] U. Struckmeier, P. Osswald, T. Kasper, L. Bohling, M. Heusing, M. Kohler, A. Brockhinke and K. Kohse-Hoinghaus, *Sampling Probe Influences on Temperature and Species Concentrations in Molecular Beam Mass Spectroscopic Investigations of Flat Premixed Low-pressure Flames*. Zeitschrift Fur Physikalische Chemie-International Journal of Research in Physical Chemistry & Chemical Physics, vol. 223, pp. 503-537, 2009.

[27] S. Dooley, F. L. Dryer, B. Yang, J. Wang, T. A. Cool, T. Kasper and N. Hansen, *An experimental and kinetic modeling study of methyl formate low-pressure flames*. Combustion and Flame, vol. 158, pp. 732-741, 2011.

[28] J. A. Miller, R. E. Mitchell, M. D. Smooke and R. J. Kee, *Nineteenth Symposium (International) on Combustion Toward a comprehensive chemical kinetic mechanism for the oxidation of acetylene: Comparison of model predictions with results from flame and shock tube experiments*. Symposium (International) on Combustion, vol. 19, pp. 181-196, 1982.

[29] A. A. Konnov, *Implementation of the NCN pathway of prompt-NO formation in the detailed reaction mechanism*. Combustion and Flame, vol. 156, pp. 2093-2105, 2009.

[30] V. A. Alekseev, M. Christensen and A. A. Konnov, *The effect of temperature on the adiabatic burning velocities of diluted hydrogen flames: A kinetic study using an updated mechanism*. Combustion and Flame, vol. 162, pp. 1884-1898, 2015.

[31] E. J. K. Nilsson and A. A. Konnov, *Role of HOCO Chemistry in Syngas Combustion*. Energy & Fuels, vol. 30, pp 2443–2457, 2016.

[32] D. L. Baulch, C. T. Bowman, C. J. Cobos, R. A. Cox, T. Just, J. A. Kerr, M. J. Pilling, D. Stocker, J. Troe, W. Tsang, R. W. Walker and J. Warnatz, *Evaluated kinetic data for combustion modeling: Supplement II*. Journal of Physical and Chemical Reference Data, vol. 34, pp. 757-1397, 2005.

[33] MATLAB R2014b ed. Mathworks, Natick, MA, US, 2001.

[34] Goos, E.; Burcat, A.; Ruscic, B. Extended Third Millenium Ideal Gas and Condensed Phase Thermochemical Database for Combustion with updates from Active Thermochemical Tables. received from Elke Goos, Elke.Goos@dlr.de April 2015.

[35] V. A. Alekseev, J. D. Naucler, M. Christensen, E. J. K. Nilsson, E. N. Volkov, L. P. H. de Goey and A. A. Konnov, *Experimental uncertainties of the heat flux method for measuring burning velocities*. Combustion Science and Technology, 2015.

[36] K. J. Bosschaart and L. P. H. de Goey, *Detailed analysis of the heat flux method for measuring burning velocities*. Combustion and Flame, vol. 132, pp. 170-180, 2003.

[37] L. P. H. de Goey, A. van Maaren and R. M. Quax, *Stabilization of Adiabatic Premixed Laminar Flames on a Flat Flame Burner*. Combustion Science and Technology, vol. 92, pp. 201-207, 1993.

[38] J. F. Yu, R. Yu, X. Q. Fan, M. Christensen, A. A. Konnov and X. S. Bai, *Onset of cellular flame instability in adiabatic CH4/O2/CO2 and CH4/air laminar premixed flames stabilized on a flat-flame burner*. Combustion and Flame, vol. 160, pp. 1276-1286, 2013.

[39] A. Bonhomme, L. Selle and T. Poinsot, *Curvature and confinement effects for flame speed measurements in laminar spherical and cylindrical flames*. Combustion and Flame, vol. 160, pp. 1208-1214, 2013.

[40] F. N. Egolfopoulos, N. Hansen, Y. Ju, K. Kohse-Höinghaus, C. K. Law and F. Qi, *Advances and challenges in laminar flame experiments and implications for combustion chemistry*. Progress in Energy and Combustion Science, vol. 43, pp. 36-67, 2014.

[41] G. Rozenchan, D. L. Zhu, C. K. Law and S. D. Tse, *Outward propagation, burning velocities, and chemical effects of methane flames up to 60 ATM*. Proceedings of the Combustion Institute, vol. 29, pp. 1461-1470, 2002.

[42] B. A. Williams, *Sensitivity of calculated extinction strain rate to molecular transport formulation in nonpremixed counterflow flames*. Combustion and Flame, vol. 124, pp. 330-333, 2001.

[43] C. M. Vagelopoulos and F. N. Egolfopoulos, *Laminar flame speeds and extinction strain rates of mixtures of carbon monoxide with hydrogen, methane,*

and air. Symposium (International) on Combustion, vol. 25, pp. 1317-1323, 1994.

[44] Y. Dong, A. T. Holley, M. G. Andac, F. N. Egolfopoulos, S. G. Davis, P. Middha and H. Wang, *Extinction of premixed H2/air flames: Chemical kinetics and molecular diffusion effects*. Combustion and Flame, vol. 142, pp. 374-387, 2005.

[45] J. Jayachandran, R. Zhao and F. N. Egolfopoulos, *Determination of laminar flame speeds using stagnation and spherically expanding flames: Molecular transport and radiation effects*. Combustion and Flame, vol. 161, pp. 2305-2316, 2014.

[46] M. Christensen, M. T. Abebe, E. J. K. Nilsson and A. A. Konnov, *Kinetics of premixed acetaldehyde + air flames*. Proceedings of the Combustion Institute, vol. 35, pp. 499-506, 2015.

[47] S. Dooley, M. P. Burke, M. Chaos, Y. Stein, F. L. Dryer, V. P. Zhukov, O. Finch, J. M. Simmie and H. J. Curran, *Methyl Formate Oxidation: Speciation Data, Laminar Burning Velocities, Ignition Delay Times, and a Validated Chemical Kinetic Model*. International Journal of Chemical Kinetics, vol. 42, pp. 527-549, 2010.

[48] Y. L. Wang, D. J. Lee, C. K. Westbrook, F. N. Egolfopoulos and T. T. Tsotsis, *Oxidation of small alkyl esters in flames*. Combustion and Flame, vol. 161, pp. 810-817, 2014.

[49] G. J. Gibbs and H. F. Calcote, *Effect of Molecular Structure on Burning Velocity*. Journal of Chemical & Engineering Data, vol. 4, pp. 226-237, 1959.

[50] N. Leplat, P. Dagaut, C. Togbé and J. Vandooren, *Numerical and experimental study of ethanol combustion and oxidation in laminar premixed flames and in jet-stirred reactor*. Combustion and Flame, vol. 158, pp. 705-725, 2011.

[51] P. Saxena and F. A. Williams, *Numerical and experimental studies of ethanol flames*. Proceedings of the Combustion Institute, vol. 31, pp. 1149-1156, 2007.

[52] G. P. Smith., D. M. Golden., M. Frenklach., N. W. Moriarty., B. Eiteneer., M. Goldenberg., C. T. Bowman., R. K. Hanson., S. Song., J. W. C. Gardiner, V. V. Lissianski. and Q. Zhiwei. Available at: http://www.me.berkeley.edu/gri_mech/

[53] A. A. Konnov, *The effect of temperature on the adiabatic laminar burning velocities of CH4−air and H2−air flames*. Fuel, vol. 89, pp. 2211-2216, 2010.

[54] P. A. Glaude, W. J. Pitz and M. J. Thomson, *Chemical kinetic modeling of dimethyl carbonate in an opposed-flow diffusion flame*. Proceedings of the Combustion Institute, vol. 30, pp. 1111-1118, 2005.

[55] P. Diévart, S. H. Won, J. Gong, S. Dooley and Y. Ju, *A comparative study of the chemical kinetic characteristics of small methyl esters in diffusion flame extinction*. Proceedings of the Combustion Institute, vol. 34, pp. 821-829, 2013.

[56] M. E. Bardin, E. V. Ivanov, E. J. K. Nilsson, V. A. Vinokurov and A. A. Konnov, *Laminar Burning Velocities of Dimethyl Carbonate with Air*. Energy & Fuels, vol. 27, pp. 5513-5517, 2013.

[57] C. K. Westbrook and F. L. Dryer, *Comprehensive Mechanism for Methanol Oxidation*. Combustion Science and Technology, vol. 20, pp. 125-140, 1979.

[58] T. S. Norton and F. L. Dryer, *Some New Observations on Methanol Oxidation Chemistry*. Combustion Science and Technology, vol. 63, pp. 107-129, 1989.

[59] T. J. Held and F. L. Dryer, *A comprehensive mechanism for methanol oxidation*. International Journal of Chemical Kinetics, vol. 30, pp. 805-830, 1998.

[60] J. Li, Z. Zhao, A. Kazakov, M. Chaos, F. L. Dryer and J. J. Scire, *A comprehensive kinetic mechanism for CO, CH2O, and CH3OH combustion*. International Journal of Chemical Kinetics, vol. 39, pp. 109-136, 2007.

[61] W. K. Metcalfe, S. M. Burke, S. S. Ahmed and H. J. Curran, *A Hierarchical and Comparative Kinetic Modeling Study of C1 − C2 Hydrocarbon and Oxygenated Fuels*. International Journal of Chemical Kinetics, vol. 45, pp. 638-675, 2013.

[62] A. Kéromnès, W. K. Metcalfe, K. A. Heufer, N. Donohoe, A. K. Das, C.-J. Sung, J. Herzler, C. Naumann, P. Griebel, O. Mathieu, M. C. Krejci, E. L. Petersen, W. J. Pitz and H. J. Curran, *An experimental and detailed chemical kinetic modeling study of hydrogen and syngas mixture oxidation at elevated pressures*. Combustion and Flame, vol. 160, pp. 995-1011, 2013.

[63] Y. Hidaka, T. Taniguchi, H. Tanaka, T. Kamesawa, K. Inami and H. Kawano, *Shock-tube study of CH2O pyrolysis and oxidation*. Combustion and Flame, vol. 92, pp. 365-376, 1993.

[64] J. Santner, F. M. Haas, F. L. Dryer and Y. Ju, *High temperature oxidation of formaldehyde and formyl radical: A study of 1,3,5-trioxane laminar burning velocities*. Proceedings of the Combustion Institute, vol. 35, pp. 687-694, 2015.

[65] V. Dias, C. Duynslaegher, F. Contino, J. Vandooren and H. Jeanmart, *Experimental and modeling study of formaldehyde combustion in flames*. Combustion and Flame, vol. 159, pp. 1814-1820, 2012.

[66] S. Wang, E. E. Dames, D. F. Davidson and R. K. Hanson, *Reaction Rate Constant of CH2O + H = HCO + H2 Revisited: A Combined Study of Direct Shock Tube Measurement and Transition State Theory Calculation*. The Journal of Physical Chemistry A, vol. 118, pp. 10201-10209, 2014.

[67] G. Friedrichs, D. F. Davidson and R. K. Hanson, *Direct measurements of the reaction H+CH2O -> H-2+HCO behind shock waves by means of Vis-UV detection of formaldehyde*. International Journal of Chemical Kinetics, vol. 34, pp. 374-386, 2002.

[68] J. Troe, *Refined Analysis of the Thermal Dissociation of Formaldehyde†*. The Journal of Physical Chemistry A, vol. 111, pp. 3862-3867, 2007.

[69] A. Laskin, H. Wang and C. K. Law, *Detailed kinetic modeling of 1,3-butadiene oxidation at high temperatures*. International Journal of Chemical Kinetics, vol. 32, pp. 589-614, 2000.

[70] G. Friedrichs, D. F. Davidson and R. K. Hanson, *Validation of a thermal decomposition mechanism of formaldehyde by detection of CH2O and HCO behind shock waves*. International Journal of Chemical Kinetics, vol. 36, pp. 157-169, 2004.

[71] W. Tsang, *Chemical kinetic data base for combustion chemistry. Part 2. Methanol*. Journal of Physical and Chemical Reference Data, vol. 16, 1987.

[72] Q. S. Li, X. Zhang and S. W. Zhang, *Direct Dynamics Study on the Hydrogen Abstraction Reaction CH2O + HO2 → CHO + H2O2*. The Journal of Physical Chemistry A, vol. 109, pp. 12027-12035, 2005.

[73] L. K. Huynh, M. Tirtowidjojo and T. N. Truong, *Theoretical study on kinetics of the H2CO + O2 → HCO + HO2 reaction*. Chemical Physics Letters, vol. 469, pp. 81-84, 2009.

[74] N. K. Srinivasan, M. C. Su, J. W. Sutherland and J. V. Michael, *Reflected Shock Tube Studies of High-Temperature Rate Constants for CH3 + O2, H2CO + O2,*

and OH + O2. The Journal of Physical Chemistry A, vol. 109, pp. 7902-7914, 2005.

[75] K. E. Noorani, B. Akih-Kumgeh and J. M. Bergthorson, *Comparative High Temperature Shock Tube Ignition of C1-C4 Primary Alcohols*. Energy & Fuels, vol. 24, pp. 5834-5843, 2010.

[76] G. Dayma, K. Hadj, K. H. Ali and P. Dagaut, *Experimental and detailed kinetic modeling study of the high pressure oxidation of methanol sensitized by nitric oxide and nitrogen dioxide*. Proceedings of the Combustion Institute, vol. 31, pp. 411-418, 2007.

[77] V. Aranda, J. M. Christensen, M. U. Alzueta, P. Glarborg, S. Gersen, Y. Gao and P. Marshall, *Experimental and Kinetic Modeling Study of Methanol Ignition and Oxidation at High Pressure*. International Journal of Chemical Kinetics, vol. 45, pp. 283-294, 2013.

[78] J. D. Naucler, L. Sileghem, E. J. K. Nilsson, S. Verhelst and A. A. Konnov, *Performance of methanol kinetic mechanisms at oxy-fuel conditions*. Combustion and Flame, vol. 162, pp. 1719-1728, 2015.

[79] R. Meana-Pañeda, D. G. Truhlar and A. Fernández-Ramos, *High-level direct-dynamics variational transition state theory calculations including multidimensional tunneling of the thermal rate constants, branching ratios, and kinetic isotope effects of the hydrogen abstraction reactions from methanol by atomic hydrogen*. The Journal of Chemical Physics, vol. 134, p. 094302, 2011.

[80] S. L. Peukert and J. V. Michael, *High-Temperature Shock Tube and Modeling Studies on the Reactions of Methanol with D-Atoms and CH3-Radicals*. The Journal of Physical Chemistry A, vol. 117, pp. 10186-10195, 2013.

[81] I. M. Alecu and D. G. Truhlar, *Computational Study of the Reactions of Methanol with the Hydroperoxyl and Methyl Radicals. 2. Accurate Thermal Rate Constants*. The Journal of Physical Chemistry A, vol. 115, pp. 14599-14611, 2011.

[82] M. Cathonnet, J. C. Boettner and H. James, *Study of methanol oxidation and self ignition in the temperature-range 500-600 °C*. Journal De Chimie Physique Et De Physico-Chimie Biologique, vol. 79, pp. 475-478, 1982.

[83] S. J. Klippenstein, L. B. Harding, M. J. Davis, A. S. Tomlin and R. T. Skodje, *Uncertainty driven theoretical kinetics studies for CH3OH ignition: HO2 + CH3OH and O2 + CH3OH*. Proceedings of the Combustion Institute, vol. 33, pp. 351-357, 2011.

[84] K. Shayan and M. Vahedpour, *Computational mechanistic study of methanol and molecular oxygen reaction on the triplet and singlet potential energy surfaces*. Structural Chemistry, vol. 24, pp. 1051-1062, 2013.

[85] R. W. Walker, A critical survey of rate constants for reactions in gas-phase hydrocarbon oxidation, in *Reaction Kinetics: Volume 1*. vol. 1, P. G. Ashmore, Ed., ed: The Royal Society of Chemistry, 1975, pp. 161-211.

[86] K. Kawamura, L. L. Ng and I. R. Kaplan, *Determination of organic acids (C1-C10) in the atmosphere, motor exhausts, and engine oils*. Environmental Science & Technology, vol. 19, pp. 1082-1086, 1985.

[87] R. W. Talbot, K. M. Beecher, R. C. Harriss and W. R. Cofer, *Atmospheric geochemistry of formic and acetic acids at a mid-latitude temperate site*. Journal of Geophysical Research: Atmospheres, vol. 93, pp. 1638-1652, 1988.

[88] E. Zervas, X. Montagne and J. Lahaye, *C-1-C-5 organic acid emissions from an SI engine: Influence of fuel and air/fuel equivalence ratio*. Environmental Science & Technology, vol. 35, pp. 2746-2751, 2001.

[89] E. Zervas, X. Montagne and J. Lahaye, *Emission of specific pollutants from a compression ignition engine. Influence of fuel hydrotreatment and fuel/air equivalence ratio*. Atmospheric Environment, vol. 35, pp. 1301-1306, 2001.

[90] E. Zervas, *Formation of organic acids from propane, isooctane and toluene/isooctane flames*. Fuel, vol. 84, pp. 691-700, 2005.

[91] F. Battin-Leclerc, A. A. Konnov, J. L. Jaffrezo and M. Legrand, *To better understand the formation of short-chain acids in combustion systems*. Combustion Science and Technology, vol. 180, pp. 343-370, 2008.

[92] N. Leplat and J. Vandooren, *Numerical and experimental study of the combustion of acetic acid in laminar premixed flames*. Combustion and Flame, vol. 159, pp. 493-499, 2012.

[93] H. Hou, B. Wang and Y. Gu, *Mechanism of the OH+CH2CO reaction*. Physical Chemistry Chemical Physics, vol. 2, pp. 2329-2334, 2000.

[94] D. L. Baulch, C. J. Cobos, R. A. Cox, C. Esser, P. Frank, T. Just, J. A. Kerr, M. J. Pilling, J. Troe, R. W. Walker and J. Warnatz, *Evaluated Kinetic Data for Combustion Modelling*. Journal of Physical and Chemical Reference Data, vol. 21, pp. 411-734, 1992.

[95] S. J. Klippenstein, J. A. Miller and L. B. Harding, *Resolving the mystery of prompt CO2: The HCCO+O2 reaction*. Proceedings of the Combustion Institute, vol. 29, pp. 1209-1217, 2002.

[96] S. A. Carl, H. Minh Thi Nguyen, R. M. I. Elsamra, M. Tho Nguyen and J. Peeters, *Pulsed laser photolysis and quantum chemical-statistical rate study of the reaction of the ethynyl radical with water vapor*. The Journal of Chemical Physics, vol. 122, p. 114307, 2005.

[97] J. P. Senosiain, S. J. Klippenstein and J. A. Miller, *Pathways and Rate Coefficients for the Decomposition of Vinoxy and Acetyl Radicals*. The Journal of Physical Chemistry A, vol. 110, pp. 5772-5781, 2006.

[98] F. De Smedt, X. V. Bui, T. L. Nguyen, J. Peeters and L. Vereecken, *Theoretical and Experimental Study of the Product Branching in the Reaction of Acetic Acid with OH Radicals*. The Journal of Physical Chemistry A, vol. 109, pp. 2401-2409, 2005.

[99] J. Mendes, C.-W. Zhou and H. J. Curran, *Theoretical Chemical Kinetic Study of the H-Atom Abstraction Reactions from Aldehydes and Acids by Ḣ Atoms and ȮH, HȮ2, and ĊH3 Radicals*. The Journal of Physical Chemistry A, vol. 118, pp. 12089-12104, 2014.

[100] V. G. Khamaganov, V. X. Bui, S. A. Carl and J. Peeters, *Absolute Rate Coefficient of the OH + CH3C(O)OH Reaction at T = 287−802 K. The Two Faces of Pre-reactive H-Bonding*. The Journal of Physical Chemistry A, vol. 110, pp. 12852-12859, 2006.

[101] L. Gasnot, V. Decottignies and J. F. Pauwels, *Kinetics modelling of ethyl acetate oxidation in flame conditions*. Fuel, vol. 84, pp. 505-518, 2005.

[102] Y. Hidaka, K. Kimura and H. Kawano, *High-temperature pyrolysis of ketene in shock waves*. Combustion and Flame, vol. 99, pp. 18-28, 1994.

[103] I. T. Woods and B. S. Haynes, *C1/C2 chemistry in fuel-rich post-flame gases: Detailed kinetic modelling*. Symposium (International) on Combustion, vol. 25, pp. 909-917, 1994.
[104] A. A. Borisov, V. M. Zamanskii, A. A. Konnov and G. I. Skachkov, Soviet Journal of Chemical Physics, vol. 6, pp. 748-755, 1990.

Summary of papers

I. Kinetics of premixed acetaldehyde + air flames

In this paper, the laminar burning velocity of acetaldehyde + air measured at atmospheric pressure and initial gas temperatures of 298-358 K were presented. The measurements were performed in non-stretched flames stabilized on the heat flux burner. The experimental data were compared with predictions of several kinetic models from the literature. The mechanism of Leplat et al., validated for acetaldehyde and ethanol oxidation, showed closest agreement with the measurements. The temperature dependence of the experimental and numerical data were investigated using the correlation $S_L = S_{L0}(T/T0)^{\alpha}$. The existence of a minimum of α in slightly rich mixtures was demonstrated experimentally and confirmed was computationally. Sensitivity analysis demonstrated that the discrepancies found between the experimental data and the simulations were a result of the sub-mechanisms of C_1 and H_2/O_2.

I planned the experimental campaign and performed the measurements together with M. T. Abebe. The data analysis and simulations were performed by me. The manuscript was written by me with contributions from my co-authors.

II. The Temperature Dependence of the Laminar Burning Velocities of Methyl Formate + Air Flames

In this paper, experimental data concerning the laminar burning velocity of methyl formate + air was presented. The measurements were performed at atmospheric pressure and initial gas temperatures of 298-348 K using the heat flux method. The temperature dependence of the laminar burning velocity was analyzed using the expression $S_L=S_{L0}(T/T_0)^{\alpha}$. The experimental data concerning both the laminar burning velocities and the α coefficients were compared with predictions obtained using mechanisms from the literature. It was demonstrated that mechanisms predicting different laminar burning velocities can have similar temperature dependence. To investigate the reactions involved in the temperature dependence, a sensitivity analysis of the α coefficient was performed for the first time. The sensitivity analysis provides insight into the temperatures sensitive reactions.

The data for this paper was acquired on two occasions 6 months apart, the first campaign was planned and performed by E.J.K Nilsson and the second one by me. All data analysis was performed by me. The manuscript was written by me with contributions from my co-authors.

III. A systematically updated detailed kinetic model for CH_2O and CH_3OH combustion

In this paper, a new detailed kinetic mechanism for formaldehyde and methanol combustion was presented. The mechanism was developed using version 0.6 of the Konnov mechanism as a starting point and had 82 reactions of the formaldehyde and methanol subset reviewed. Rate constants were selected based on thorough evaluation of available experimental and theoretical data and accepted as published with no modifications. The mechanism was validated over a wide range of experimental conditions and devices including shock tube and flow reactors as well as both burner stabilized and freely propagating flames with an overall good agreement. The new mechanism showed a significant improvement in predicting the laminar burning velocity of methanol as compared to version 0.6.

E.J.K Nilsson and I developed the kinetic mechanism. Validation of the mechanism was performed by me. The manuscript was written by me with contributions from my co-authors.

IV. Laminar burning velocity of acetic acid + air flames

In this paper, experimental data concerning the laminar burning velocity of acetic acid + air measured at atmospheric pressure and initial gas temperatures of 338-358 K was presented. The measurements were performed using the heat flux method. Experimental challenges that arise due to the corrosiveness of acetic acid towards the brass burner plate resulted in larger uncertainties than working with non-corrosive substances. A recently developed methanol and formaldehyde mechanism, presented in Paper III, was extended with 70 reactions to acetic acid combustion. The new mechanism was compared with the laminar burning velocities and species profiles of a burner stabilized acetic acid flame. The mechanism overpredicted the laminar burning velocities by approximately 3 cm/s. The simulated species profiles of a burner stabilized flame were in good agreement to experimental data of major products, minor intermediates were over- or under-predicted by the model. To investigate reactions responsible for the deviation of the mechanism, sensitivity analysis was used. It was found that the calculated burning velocities were insensitive to fuel specific reactions and mostly governed by C_1 chemistry (typical for hydrocarbons) and

reactions of ketene. Possible modifications of the rate constants within the evaluated uncertainty factors were discussed.

The experimental study was planned and carried out by me. I also processed the data. The sub mechanism of acetic acid was developed by Prof. A.A Konnov. Validation of the mechanism was made in collaboration between me and Prof. A.A Konnov. The manuscript was largely prepared by Prof. A.A Konnov with contributions from me.